



HAL
open science

Effects of natural wing damage on flight performance in Morpho butterflies: what can it tell us about wing shape evolution?

Camille Le Roy, Raphael Cornette, Violaine Llaurens, Vincent Debat

► To cite this version:

Camille Le Roy, Raphael Cornette, Violaine Llaurens, Vincent Debat. Effects of natural wing damage on flight performance in Morpho butterflies: what can it tell us about wing shape evolution?. *Journal of Experimental Biology*, 2019, 222 (16), pp.jeb204057. 10.1242/jeb.204057 . hal-02114273v2

HAL Id: hal-02114273

<https://hal.science/hal-02114273v2>

Submitted on 12 Sep 2019

HAL is a multi-disciplinary open access archive for the deposit and dissemination of scientific research documents, whether they are published or not. The documents may come from teaching and research institutions in France or abroad, or from public or private research centers.

L'archive ouverte pluridisciplinaire **HAL**, est destinée au dépôt et à la diffusion de documents scientifiques de niveau recherche, publiés ou non, émanant des établissements d'enseignement et de recherche français ou étrangers, des laboratoires publics ou privés.

1 Effects of natural wing damage on flight performance in *Morpho*
2 butterflies: what can it tell us about wing shape evolution?

3 Camille Le Roy^{1,2,*}, Raphaël Cornette¹, Violaine Llaurens^{1†} and Vincent Debat^{1†}

4
5 ¹Institut de Systématique, Evolution, Biodiversité (ISYEB), Muséum National d'Histoire
6 Naturelle, CNRS, Sorbonne Université, EPHE, Université des Antilles, CP50, 75005, Paris,
7 France. ²Université Paris Descartes, Sorbonne Paris Cité, 12 rue de l'École de Médecine,
8 75006, Paris, France.

9
10 * Author for correspondence (leroy.camille7@gmail.com)

11 †Equal contribution

12
13 **ABSTRACT**

14 Flying insects frequently experience wing damage during their life. Such irreversible alterations
15 of wing shape affect flight performance and ultimately fitness. Insects have been shown to
16 compensate for wing damage through various behavioural adjustments, but the importance of
17 damage location over the wings has been scarcely studied. Using natural variation in wing
18 damage, here we tested how the loss of different wing parts affect flight performance. We
19 quantified flight performance in two species of large butterflies, *Morpho helenor* and *M. achilles*,
20 caught in the wild, and displaying large variation in the extent and location of wing damage. We
21 artificially generated more severe wing damage in our sample to contrast natural *vs.* higher
22 magnitude of wing loss. Wing shape alteration across our sample was quantified using geometric
23 morphometrics to test the effect of different damage distributions on flight performance. Our
24 results show that impaired flight performance clearly depends on damage location over the
25 wings, pointing out a relative importance of different wing parts for flight. Deteriorated
26 forewings leading edge most crucially affected flight performance, specifically decreasing flight
27 speed and proportion of gliding flight. In contrast, most frequent natural damage such as scattered
28 wing margin had no detectable effect on flight behaviour. Damages located on the hindwings –
29 although having a limited effect on flight – were associated with reduced flight height, suggesting
30 that fore- and hindwings play different roles in butterfly flight. By contrasting harmless and
31 deleterious consequences of various types of wing damage, our study points at different selective
32 regimes acting on morphological variations of butterfly wings.

33
34 Keywords: Wing morphology, behaviour, geometric morphometrics, aerodynamics, Lepidoptera.

35

A Figure 5A

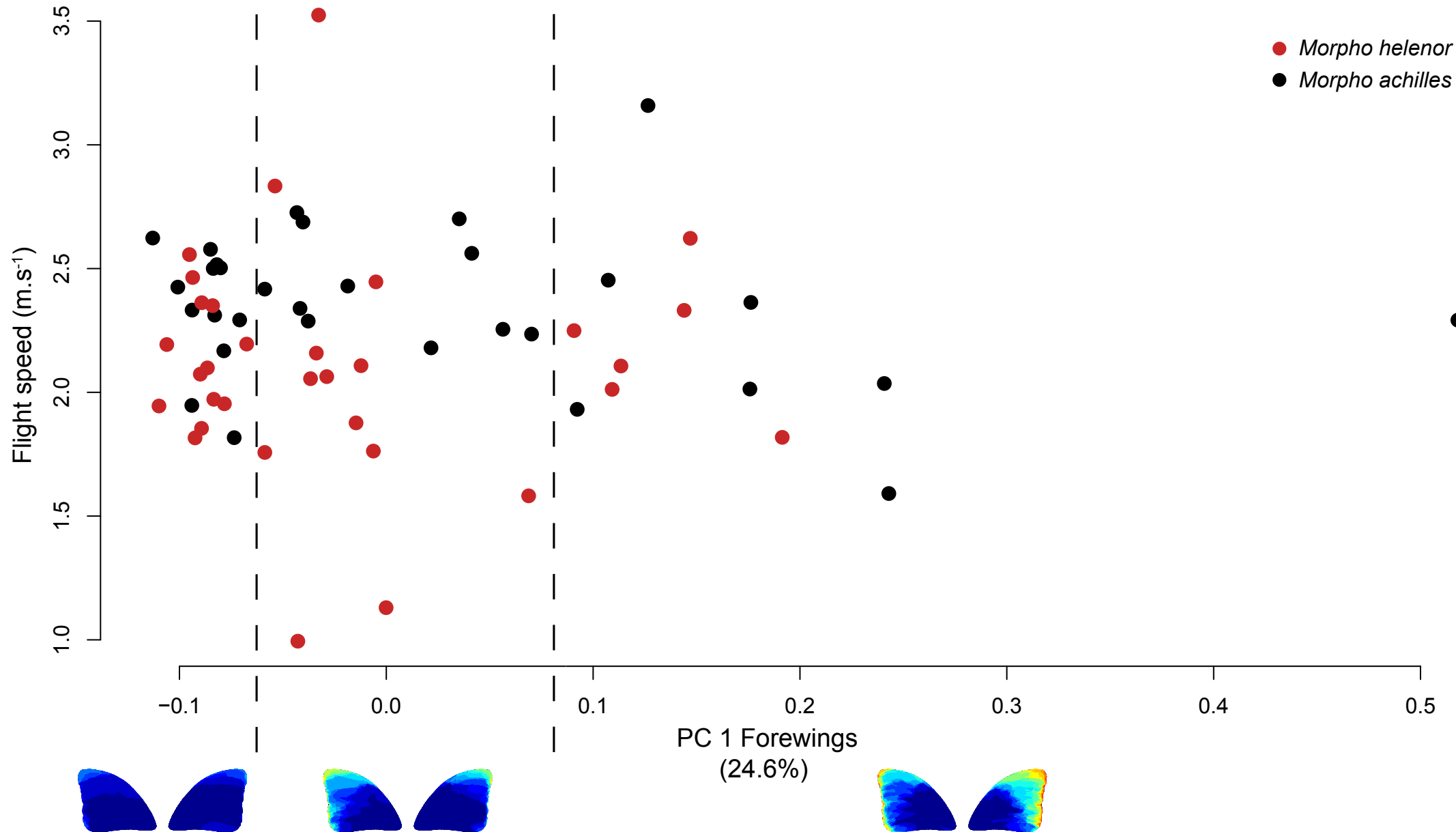


Figure 4

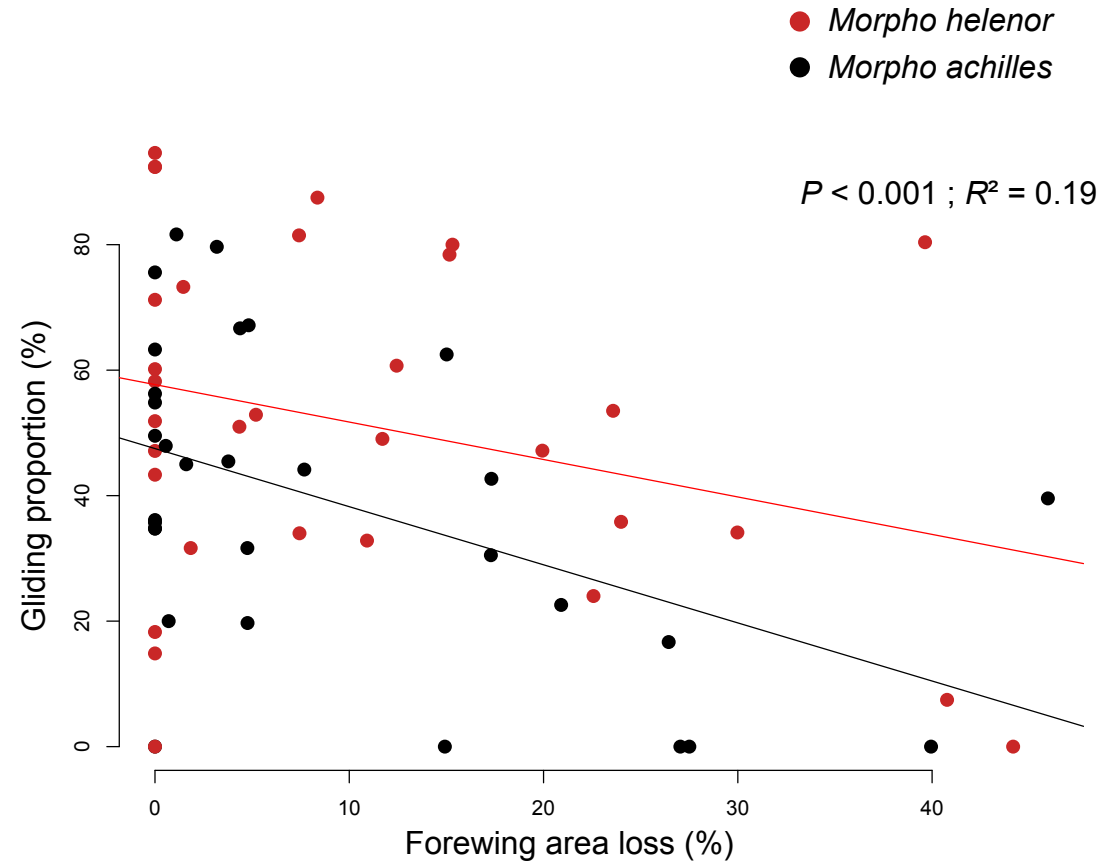
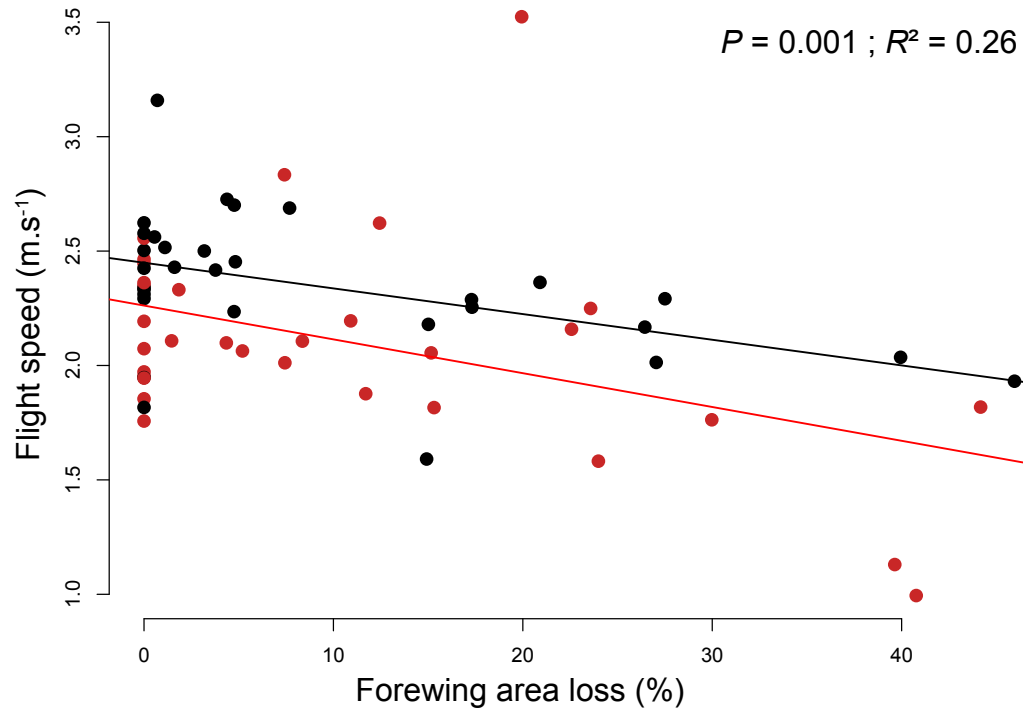


Figure 3B

B

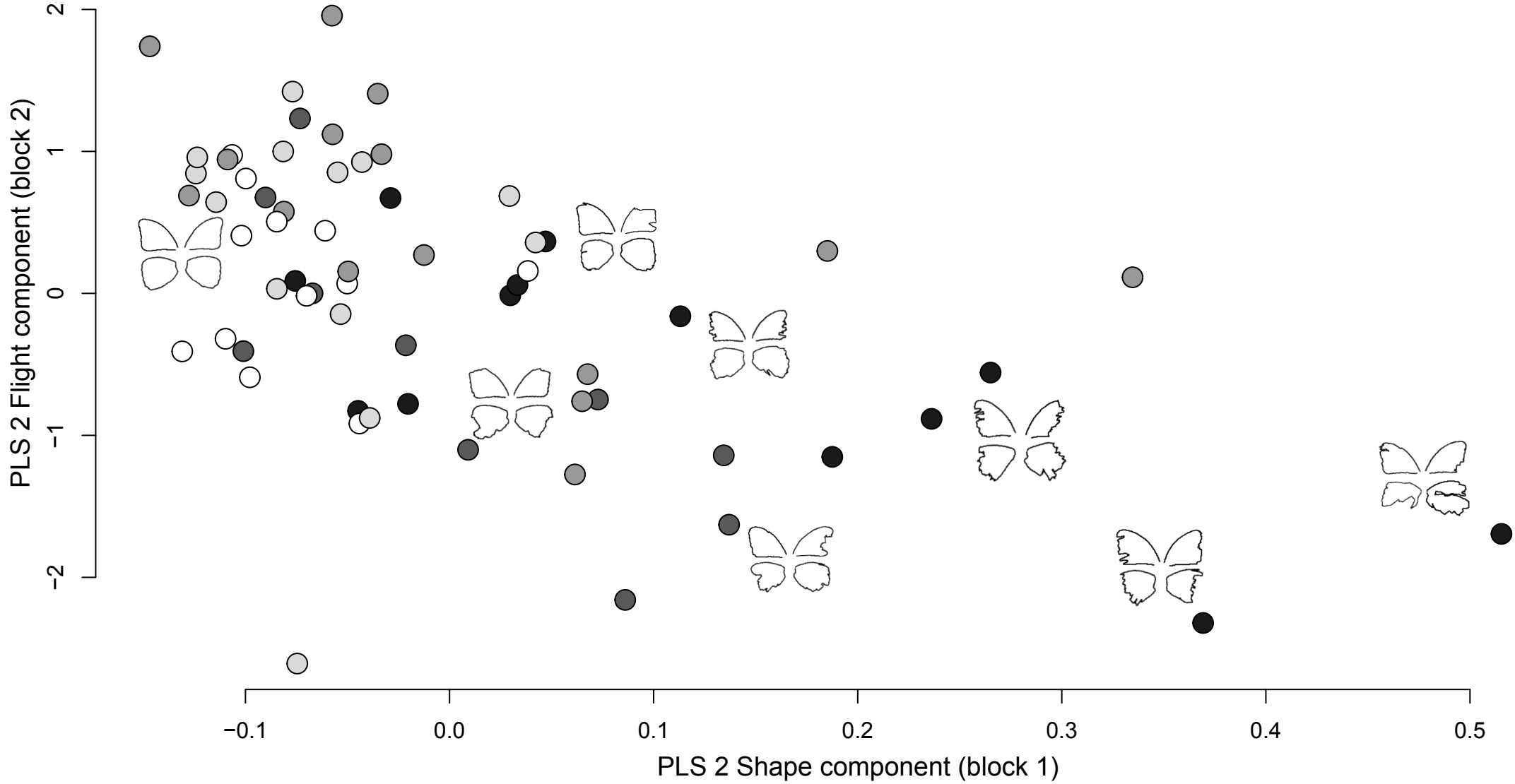


Figure 3A

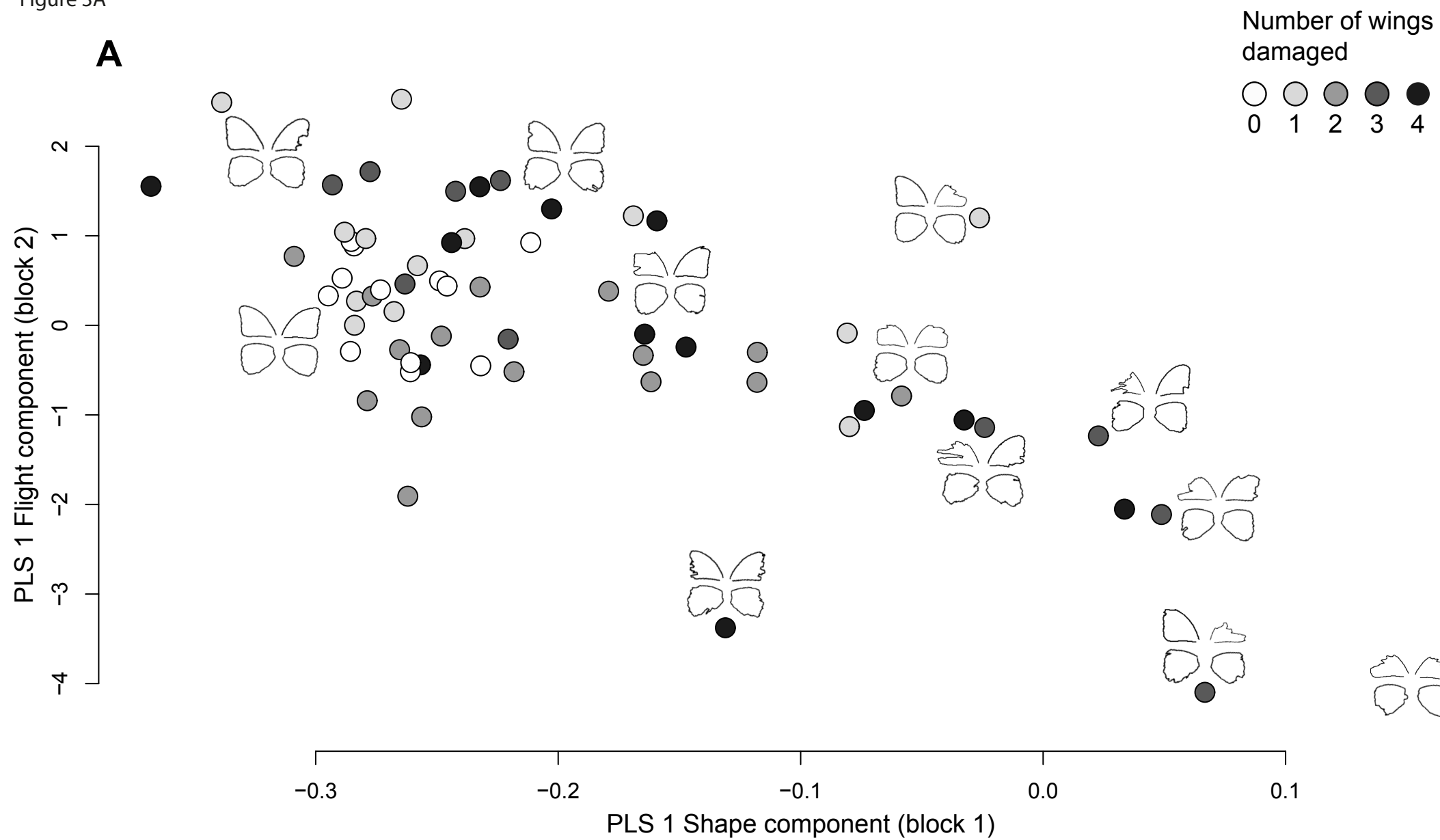
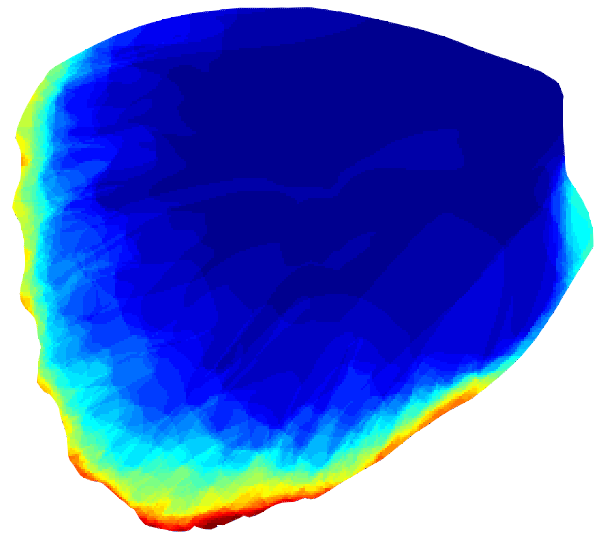
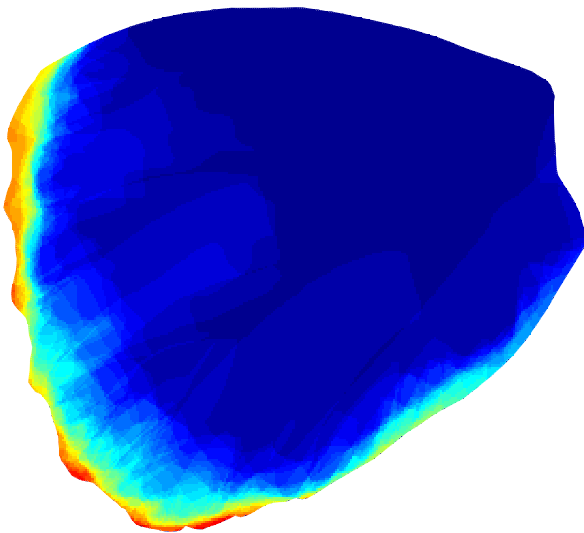
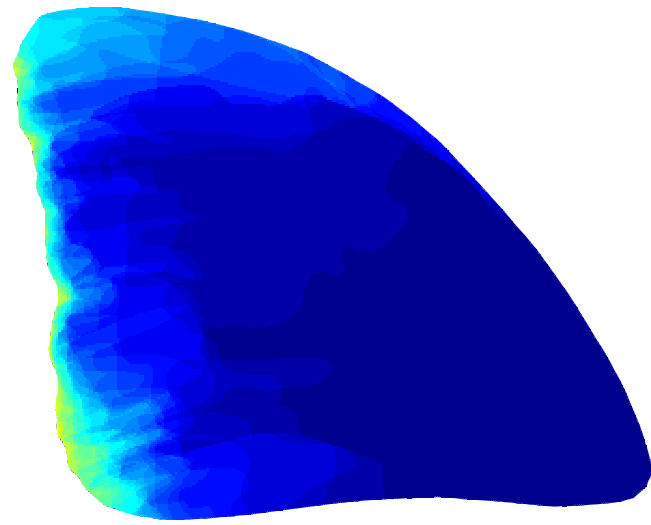
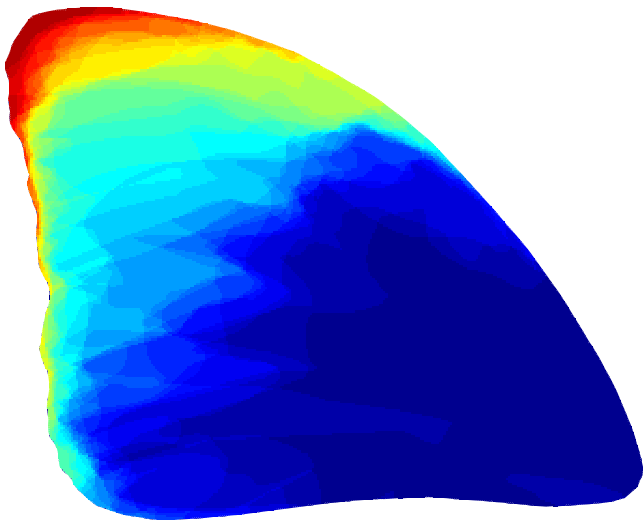


Figure 2

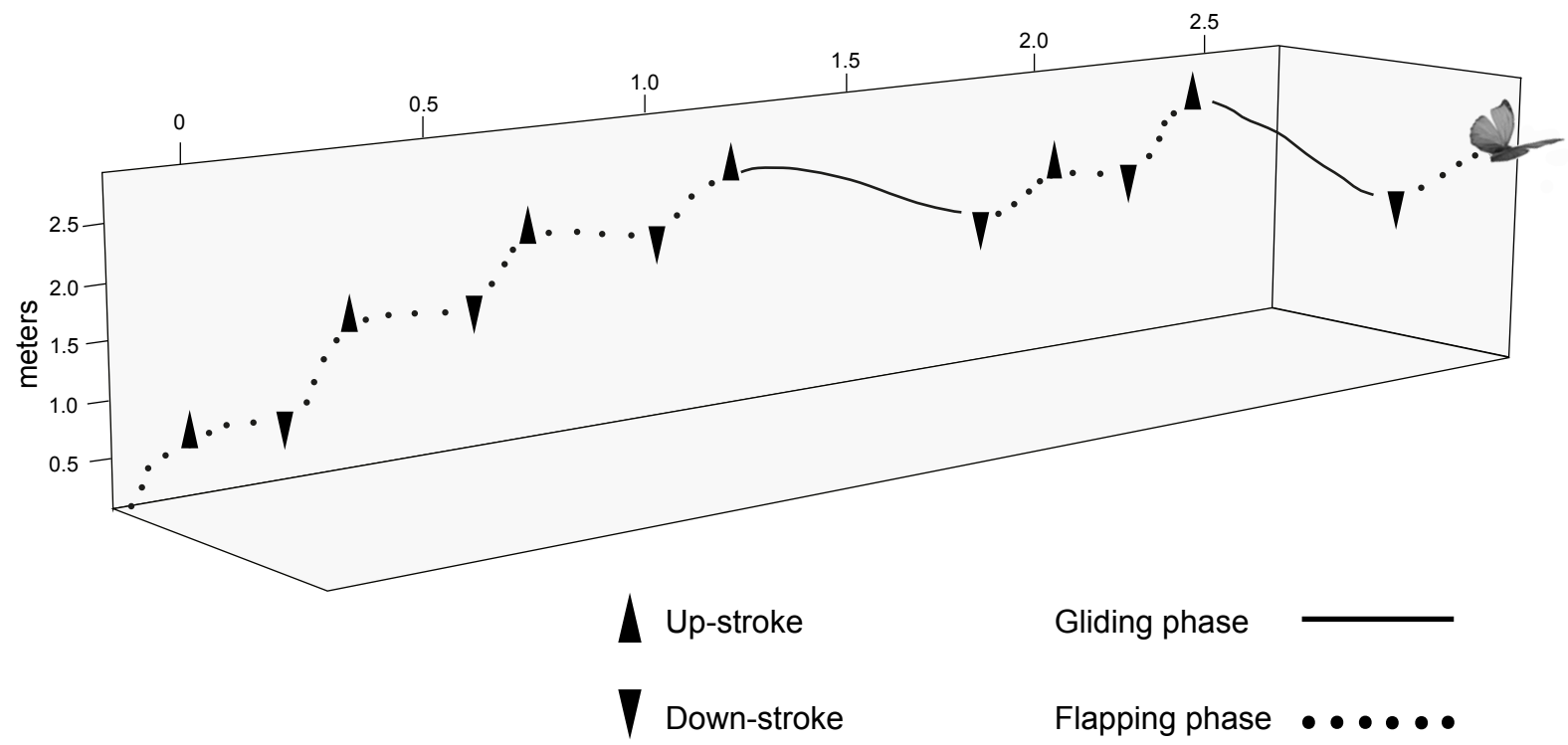
Cage
N = 25 ind.

Nature
N = 38 ind.



1 ind.  21 ind.

Figure 1



36

37 **INTRODUCTION**

38 Understanding the evolution of wing morphology requires estimating the impact of wing shape
39 variations on fitness-related behaviours. In butterflies, flying capacities enabled by wing
40 morphology are crucial throughout adult life during many key behaviours involved in survival,
41 such as resource foraging (Hall and Willmott, 2000) or escaping from predators (Barber et al.,
42 2015; Chai and Srygley, 1990), and in reproduction, such as male-male contest (Berwaerts et al.,
43 2006; Wickman, 1992) or courtship (Scott, 1974). Wing shape directly affects various aspects of
44 flight performance, ranging from the energy budget (Ancel et al., 2017) to the aerodynamic
45 forces produced during wingbeats (Ellington, 1984; Muijres et al., 2017). Investigating the
46 consequences of wing shape variations on these different components of flight performance may
47 shed light on the forces driving wing shape evolution within and across species (Arnold, 1983;
48 Norberg and Rayner, 1987; Le Roy et al., 2019). For example, selection acting on wing shape has
49 been evidenced by comparing migrating and non-migrating populations of monarch butterflies:
50 migrating individuals exhibit more elongated wing shape, likely reducing flight cost and hence
51 benefiting to their long distance migration (Altizer and Davis, 2010; Dockx, 2007). However, the
52 consequences of wing shape variation on flight performance are poorly documented, preventing
53 the precise identification of the selective pressures acting on wing shape evolution (Chazot et al.,
54 2016; Johansson et al., 2009; Outomuro and Johansson, 2015).

55 To investigate the effect of wing shape variation on flight performances, most previous studies
56 have performed experimental manipulations of wing shape. For example, experimental wing
57 clipping in butterflies has allowed highlighting the importance of hindwings for linear and
58 turning acceleration in Lepidoptera (Jantzen and Eisner, 2008). Artificially-modified wings have
59 mainly been used to investigate how insects compensate for such a loss by altering their
60 behaviour. The loss of wing surface has been shown to induce an increase of wingbeat frequency
61 in bees (Hedenström et al., 2001; Vance and Roberts, 2014), flies (Muijres et al., 2017) and
62 butterflies (Kingsolver, 1999). In hawkmoth, asymmetrical wing loss cause the insect to flap its
63 damaged wing with a larger amplitude, correcting for the unequal force production (Fernández et
64 al., 2012). In flies, the compensation of asymmetrical wing loss involves a body roll towards the
65 damaged wing and changes in wing motion (Muijres et al., 2017). Although behavioural
66 adjustments in response to wing damage may have evolved in some insects, a significant fitness

67 cost of wing damages has nevertheless been documented in some studies. Field studies on
68 bumblebees have shown a reduced foraging efficiency in damaged individuals (Higginson and
69 Barnard, 2004) as well as a lower life expectancy (Cartar, 1992). In dragonflies, reduction of
70 hindwing area significantly decreases capture success (Combes et al., 2010). In butterflies
71 however, a mark-recapture study found no effect of wing surface reduction on survival
72 (Kingsolver, 1999).

73 In the studies mentioned above, wing alterations were typically generated by clipping the
74 wings, and usually consisted in symmetric vs. asymmetric reduction of wings' surface (Fernández
75 et al., 2012; 2017; Haas and Cartar, 2008; Vance and Roberts, 2014), or gradual reduction in
76 wings surface (Muijres et al., 2017; Vance and Roberts, 2014). But these artificial alterations may
77 not reflect the natural wing damage experienced by insects in the wild. The spatial distribution
78 and extent of damages on wings of wild insects have rarely been quantified in natural populations
79 (but see Higginson and Barnard, 2004). In the wild, a frequent source of wing damage is collision
80 with obstacles (Foster and Cartar, 2011). Accidental collisions may rip the wing in various extent
81 and directions, although somewhat constrained by the veins architecture (Mountcastle and
82 Combes, 2014; Wootton, 1992). Collisions may also occur during agonistic interactions with
83 conspecifics (Alcock, 1996; Carvalho et al., 2016). Failed predators attacks can also cause
84 significant damage in different wing locations (Carpenter, 1942; Edmunds, 1974; Robbins, 1981;
85 Shapiro, 1974). As a result, flying insects have to cope with a wide diversity of damage during
86 their life, varying both in their extent and location. While some damage may have too harsh
87 consequences on flight to even be observable in the wild, most frequently observed damages are
88 probably less deleterious, or more easily compensable. Studying wing damages in wild-caught
89 individuals, that probably have a limited impact on survival capacities, should allow
90 characterizing wing shape variations with a diversity of effects on fitness, from neutral to
91 severely deleterious. This situation is therefore relevant to investigate the consequences on flight
92 of a biologically realistic range of damage, as a step towards inferring the selective pressures
93 acting on wing shape.

94 In this study we used natural and artificially-accentuated damages on butterfly wings to test
95 how modifications of different wings, and different wing areas, affect flight performance. We
96 studied wild-caught individuals of two species of large butterflies, *Morpho helenor* and *M.*
97 *achilles* (Nymphalidae, Satyrinae), exhibiting a large variation in wing damage. We first

98 quantified their flight performance using three-dimensional videography. We then precisely
99 determined the frequency and spatial location of damage over the four wings using geometric
100 morphometrics, allowing to estimate and compare the effects of natural and artificially-
101 accentuated damages on flight performance. Although the initial cause of wing damage in the
102 wild is not known, our study captures part of the range of naturally occurring wing shape
103 alteration. The reported effects on flight performance are thus expected to reflect typical
104 challenges that butterflies face in the wild throughout their adult life. By generating more severe
105 wing damage in our sample, we aimed at contrasting natural – presumably non-lethal – damage,
106 with damage of higher magnitude that would more strongly threaten survival in the wild.

107

108 **MATERIALS AND METHODS**

109 **Study sites and sampled specimens**

110 Field sampling was performed in July and August 2016, in the middle basin of the Río Huallaga
111 (San Martín Department, Peru), near the city of Tarapoto, along the Rio Shilcayo (06°27'07''S,
112 76°20'47''W; ca. 450m) and the village of San Antonio de Cumbasa (06°24'24''S, 76°24'25''W;
113 ca. 470m). We sampled a total of 63 *Morpho*, including 32 individuals from the species *Morpho*
114 *helenor* and 31 from the species *M. achilles*. These two species are nearly identical
115 phenotypically (Blandin, 1988) and are thought to have similar flight behaviours (DeVries et al.,
116 2010). Only three females were caught, largely due to their cryptic flight behaviour, contrasting
117 with the extensive patrolling displayed by males. Half of the captured specimens was undamaged,
118 while the remaining had their wings at least slightly damaged. In order to increase the variation of
119 wing damage in our sample, 25 of the captured specimens were stored in a mesh-cage
120 (4m×2m×1.8m) during 3 days, so as to generate collision-induced wing damage. The final
121 sample was composed 31 undamaged individuals and 32 individuals for which damage extent
122 ranged from little to half of missing wing surface. Out of the 32 damaged individuals, 13 came
123 from the wild and 19 from the cage.

124

125 **Filming**

126 Butterflies were filmed in a large outdoor insectary (8m×4m×2.5m) built close to the sampling
127 sites, in a sheltered spot where no wind was detectable. Each specimen was released from a
128 shaded side of the cage, and generally flew towards the sunniest part of the cage. Two video

129 cameras (GoPro Hero4Black set at 60 images per second) mounted on a tripod at fixed height
130 were used to record the films. In order to capture most of the flight path, camera zoom lens were
131 set on wide angle (focal length: 14 mm) thereby allowing to cover the entire volume of the cage
132 when combining the two cameras views. A successful sequence was defined as a flight path
133 moving through the entire field of view of the two cameras. Multiple trials were performed until a
134 minimum of three successful sequences were obtained for each individual. We recorded a total of
135 227 successful sequences with a mean duration of 1.4 ± 0.89 seconds, ranging from 0.6 to 6.8
136 seconds. After being filmed, specimens were placed in a -20°C freezer, ensuring subsequent
137 morphological measurements to exactly match the state in which butterflies have flown.

138

139 **Flight analysis**

140 Sequences of the same flight obtained from the two cameras were first synchronized with respect
141 to a reference frame. The frame distortion (Fisheye effect) due to wide angle settings was
142 corrected without limiting the wide view angle, using DWarp Argus package (Jackson et al.,
143 2016) implemented in Python2.7. To recover exact distances from films, cameras were calibrated
144 with the Direct Linear Transformation (DLT) technique (Hartley and Sturm, 1995; Kwon, 1998)
145 by digitalizing an object of known length (here a wand) moved throughout the experimental cage.
146 The wand tracking and DLT coefficient computation were performed using DLTdv5 (Hedrick,
147 2008) and easyWand (Theriault et al., 2014) Matlab program respectively. To facilitate the
148 tracking of the filmed butterflies, a background subtraction algorithm (KaewTraKulPong and
149 Bowden, 2002) was applied to each video via Python2.7. Trajectory points were digitalized for
150 each frame at the centroid of the butterfly. Wingbeats were quantified by manually digitizing a
151 point on the butterfly within frames containing the highest up-stroke positions and those
152 containing the lowest down-stroke positions, transcribing the spatial and temporal position of
153 each wing stroke along the flight trajectory (Fig. 1). Based on the temporal wing stroke position,
154 gliding flight phases along the trajectory were defined as at least 10 consecutives frames
155 (representing 0.16 seconds) without any wing stroke. The other parts of the trajectory were
156 considered as flapping phases (Fig. 1). By reducing wing surface, wing damages can limit the
157 gliding capacities of the observed butterflies: this can be behaviourally compensated by a
158 reduction in the length of gliding phases and/or an increase in wing beat frequencies during the
159 flapping phases. To distinguish those two behavioural compensations we computed both the total

160 wing beat frequency through time and the wing beat frequency within flapping phases.

161 Flight trajectories were then smoothed using a low pass Butterworth filter (order = 4; critical
162 frequency = 0.5) (Butterworth, 1930), removing the high frequency movements, *i.e.* the steep
163 gaps – artefactual movements within trajectories, stemming from tracking noise (see
164 Supplementary figure S1). Using a custom-written R script, we calculated the following
165 parameters for each flight trajectory: flight velocity, sinuosity (computed as the ratio of the actual
166 distance covered over the distance between starting and ending position), wingbeat frequency,
167 gliding proportion and flight height. These non-redundant parameters were chosen for their
168 relevance in describing flight behaviour. They were computed as the mean value over the flight
169 trajectory. We also extracted the maximal duration of gliding and flapping phases, and the
170 smallest turning angle of each trajectory as a measure of manoeuvrability (Rayner, 1988). We
171 summarized the flight performance of each individual by retaining the mean and max values out
172 of the three flight sequences analysed per individual.

173

174 **Capturing spatial variation in wing damage**

175 Fore- and hindwings were photographed in dorsal view using NikonD90 camera in controlled
176 light conditions. The spatial variation of damages within and between wings, but also between
177 naturally and artificially damaged individuals, was visually assessed by generating a heat map
178 (Fig. 2, see also Fig. S2 and S3). This was done by superimposing standardized images of the
179 wings from all specimens using EBImage R package (Pau et al., 2010) so as to count the missing
180 area at the pixel-scale. The heat map was built from a matrix summing the occurrences of missing
181 pixels, and plotted with autoimage R package (French, 2017).

182 As our goal was to capture the different distribution of damages throughout the wings, we
183 considered damage variation as a wing shape alteration, and quantified it using a landmark-based
184 geometric morphometric method (Adams et al., 2004; Bookstein, 1997). This method has proven
185 well-suited for studying variations in butterfly wing shape and venation (e.g. Breuker et al., 2010;
186 Chazot et al., 2016; Zhong et al., 2016), albeit never used to quantify variation in wing damage.
187 Because the extent of vein architecture available differed between specimens depending on wing
188 damage, we did not place fixed landmarks on the vein architecture. We used 300 semi-landmarks
189 equidistantly spaced along the (more or less damaged) wing outline. Semi-landmarks can be used
190 when identifiable landmarks are unavailable. To remove the variation along the outline due to a

191 lack of homology, the semi-landmarks are allowed to slide along the local tangent to the curve in
192 an iterative process (Gunz and Mitteroecker, 2013). Once slid, they can be treated as regular
193 landmarks in the analyses. We also placed one fixed landmark at the wing base, fixing the overall
194 landmarks configuration with respect to this homologous position available for all specimens.
195 The procedure was applied to both the left and right-reflected forewings and hindwings. All
196 landmarks were digitized using TpsDig2 (Rohlf, 2015).

197 In order to obtain variables describing shape alteration between specimens, we then performed
198 a General Procrustes Analysis (Rohlf and Slice, 1990) on the landmarks configurations of each of
199 the 4 wings using geomorph R package (Adams and Otárola-Castillo, 2013). This procedure
200 extracts the shape information from landmarks positions by getting rid of the extraneous
201 variations, namely, the position, size and orientation (Adams et al., 2004). Variation in the newly
202 obtained Procrustes coordinates then only reflects shape variation. Because our goal was to relate
203 wing shape alteration to that measured in flight parameters, it was necessary to analyse
204 simultaneously both pairs of wings. Indeed, the observed flight results from the combined use of
205 the four wings, and is therefore potentially affected by their combined shape alteration. After each
206 wing was superimposed separately, we conducted a Principal Component Analysis (PCA) on
207 each sets of Procrustes coordinates. We then combined the PCs accounting for 90% of cumulated
208 variance of each of these four PCAs. Finally, we performed a new PCA on this global dataset to
209 obtain PCs that combine the shape information of the four wings per individual (Fig. S4). We also
210 applied this procedure independently on the forewings and hindwings to focus on the effect of
211 their respective shape alteration on flight separately.

212

213 **Quantifying damage extent**

214 Wing area was computed from the previously digitalized landmarks using Momocs R package
215 (Bonhomme et al., 2014) independently on each of the 4 wings. Wing area was preferred over
216 other measures of size (e.g. centroid size): it is indeed directly relevant for aerodynamics and was
217 found less affected by extreme irregularities in outlines. For specimens with only the left (or
218 right) wing damaged, damage extent was calculated by subtracting the area of its right (or left)
219 damaged wing to the area of its intact counterpart. When specimens had their two wings
220 damaged, we used the mean wing area of the intact specimens. Damage extent was expressed
221 separately for the fore and hindwings to test their respective effect on flight performance. We also

222 computed the asymmetry resulting from wing damage, expressed as the absolute value of the
223 difference in damage extent between the right and left sides of the specimen.

224

225 **Statistical analyses**

226 All statistical analyses were conducted in R (Team, 2013). We first tested the effect of species
227 and sex on flight parameters, while considering only undamaged specimens, using multivariate
228 analysis of variance (MANOVA). Variation in flight performances was examined by performing a
229 PCA on the set of flight parameters (Fig. S5). Principal components (PCs) are linear
230 combinations of the original data that maximize the variation between individuals. The first PCs,
231 accounting for the major trends in flight variation, were then used as flight data in the subsequent
232 multivariate analyses. The covariation between wing damage and flight was first assessed by
233 Escoufier's RV coefficient (Escoufier, 1973; Klingenberg, 2009). We then performed a two-
234 blocks partial-least squares (2B-PLS) regression between flight and shape datasets. The 2B-PLS
235 analysis specifically focuses on the covariation between two sets of multivariate data, by
236 constructing pairs of linear combinations of variables within each dataset (here the shape and
237 flight PCs) that maximally covary across datasets (Rohlf and Corti, 2000). Then in order to
238 identify the precise effect of area loss on flight behaviour, we tested the effect of fore- and
239 hindwings area loss and their asymmetry on each flight parameter, using multiple regression
240 analysis. Species, sex and cause of damage (*i.e.* cage or nature) were included as factors to
241 control for their respective effects on flight.

242 To test for the effects of the distribution of damage on flight performances, we performed
243 multiple regressions of the shape PCs on each flight parameters. Finally, because the PCs are
244 composite variables combining information on different wings, direct visualization of the
245 associated morphologies is not straightforward. To visualize damage variations explained by the
246 different PCs, we separated individuals into three groups of equal size (first, second and last
247 third) depending on their location along the PCA axis, and used the heat maps to depict damage
248 variation within each group (Fig. 5).

249

250 **RESULTS**

251 **Extent and location of wing damage**

252 The extent of damage within our sample ranged from 0 to 39.49% of missing wing area at the

253 individual level, with up to 45.96% and 51.46% for the forewings (FW) and hindwings (HW)
254 respectively. Wing asymmetry was strongly correlated with damage extent ($r = 0.72$; $P < 0.001$),
255 highlighting that wing damage rarely occurred symmetrically. Damage proportion between FW
256 and HW was not correlated ($r = 0.15$; $P = 0.31$) but both wings were on average similarly
257 affected (mean damage extent = $13.37 \pm 1.90\%$ on FW vs. $10.68 \pm 1.75\%$ on HW; $P = 0.37$; $W =$
258 1222). Individuals kept in cage were more damaged relative to those damaged in nature. This
259 difference was mostly due to larger damage on the forewings in individuals kept in cage
260 ($P < 0.001$; $W = 0.76$ vs. $P = 0.05$; $W = 616$ when comparing forewings and hindwings damage
261 respectively). It should be noted, however, that wing damages produced in the cage may have
262 added to natural damage for which we have no record. Types of damage were nevertheless
263 different between individuals from cage and those from nature. Collisions occurring in cage
264 mostly affected the leading edge of the forewings. In contrast, the most frequent natural damages
265 were located along the marginal and posterior zone of the hindwing (Fig. 2).

266

267 **Effect of wing damage on flight performance**

268 As similar results were found when using either the mean or the maximal values of flight
269 parameters, only the maximal values are considered below. Amongst all flight parameters
270 computed, only gliding proportion and longest gliding phase were strongly correlated ($r > 0.50$):
271 we thus excluded the longest gliding phase from the analysis. The MANOVA performed on
272 undamaged individuals revealed no difference among species on flight parameters (Wilks'
273 $\lambda = 0.854$; $P = 0.52$). Although our sample included only two undamaged females, an effect of
274 sex was detected on flight speed: female flight was significantly slower than male's ($P < 0.05$;
275 $W = 54$).

276 Covariation between wing shape and flight parameters was significant (RV-coefficient = 0.20;
277 $P = 0.01$). The first PLS vector (53.87% of covariation explained) carried a variation in flight
278 parameters (PLS1 block 2) opposing higher flight speed and gliding proportion to longer flapping
279 phases duration and higher wingbeat frequency (Tab. 1). This was associated with the shape
280 component (PLS1 block 1) describing an accumulation of wing damage mostly located on the
281 forewings (Fig. 3). This covariation was clearly driven by severely damaged individual, as both
282 intact and slightly damaged individuals displayed similar variation in flight parameters. Another
283 pattern of covariation was detected on the second PLS axis (21.33% of covariation explained),

284 where most of the flight variation was driven by the flight height, and associated with variation in
 285 wing damages located on the hindwings.

286 When running multiple regression analysis, we found that the effect of wing area loss on flight
 287 parameters was not affected by sex ($P = 0.91$), nor by the cause of damage (i.e. cage vs. nature;
 288 $P = 0.50$). Although no effect of species was detected on flight parameters among undamaged
 289 individuals (*M. helenor*: $n = 14$; *M. achilles*: $n = 17$), a significant effect of species was detected
 290 on flight speed ($P < 0.05$) and gliding proportion ($P < 0.05$) when testing for the effect of wing
 291 damage on flight. Controlling for the species effect, we found that forewings area loss had a
 292 significant negative effect on flight speed ($R^2 = 0.26$, $F_{60,0.35} = 10.69$, $P < 0.001$) and gliding
 293 proportion ($R^2 = 0.19$, $F_{60,24.09} = 7.10$, $P < 0.001$). Specifically, *M. achilles* and *M. helenor* both
 294 flew slower as their forewings were damaged, although for the same degree of damage, *M.*
 295 *helenor* reduced its normal flight speed by 19% ($0.43 \text{ m}\cdot\text{s}^{-1}$) while *M. achilles* only reduced it by
 296 13% ($0.32 \text{ m}\cdot\text{s}^{-1}$). Similarly, the extent of gliding flight decreased as forewings damages increased
 297 for both species, but *M. achilles* reduced its gliding proportion by 59% while *M. helenor* only
 298 reduced it by 32% for a same degree of damage (Fig. 4). A slight increase in wingbeat frequency
 299 was associated with forewing area loss ($R^2 = 0.11$, $F_{60,1.2} = 3.67$, $P < 0.05$), but such effect was
 300 not detected when focusing only on flapping phases ($R^2 = 0.05$, $F_{60,2.1} = 1.63$, $P = 0.50$),
 301 consistent with a transition from flap-gliding flight to continuous flapping flight associated with
 302 forewing damage. Forewings area loss was indeed positively associated with maximal flapping
 303 duration ($R^2 = 0.23$, $F_{61,0.57} = 18.67$, $P < 0.001$). Hindwings area loss did not contribute to explain
 304 variation in the previous flight parameters, but had a significant – negative effect on flight height
 305 ($R^2 = 0.08$, $F_{61,0.26} = 5.65$, $P < 0.05$). No effect of wing asymmetry was detected, probably
 306 because it was strongly correlated with wing area loss.

307 **Tab. 1. Correlation coefficients between flight parameters and the flight component of PLS 1 and PLS2.**

	Flight speed	Flapping duration	Wingbeat frequency	Flight height	Gliding proportion	Sinuosity	Smallest angle
Flight component PLS 1	0.52	-0.90	-0.58	-0.20	0.63	-0.19	0.23
Flight component PLS 2	-0.01	0.30	0.46	0.92	-0.11	0.00	-0.05

r-value > 0.5 in bold.

309
310 The different types of damage distribution captured by the shape PCs had contrasted effects on
311 flight parameters. In particular, the reduction in flight speed and the extension of flapping phase
312 durations were explained by forewing shape alteration described on the PC2 ($R^2 = 0.18$,
313 $F_{61,0.37} = 13.61$, $P < 0.001$ and $R^2 = 0.22$, $F_{61,0.58} = 17.71$, $P < 0.001$ respectively). These two
314 flight parameters were negatively correlated ($r = -0.41$; $P < 0.001$): most damaged individuals
315 had both a reduced flight speed and used nearly only flapping flight. In contrast to the forewing
316 shape variation carried on the PC2, variation on PC1 showed no relationship with flight variation,
317 neither did any PC carrying hindwings shape variation. The distribution of damages throughout
318 the wings shown by the heat maps revealed that damages located at the forewing tips (shape
319 variation on PC2) were associated with reduced flight speed. Damages occurring along forewing
320 margin in contrast, show no effect on variation in flight speed (Fig. 5).

321

322 **DISCUSSION**

323 **Kinematic response to wing damage**

324 Our results show that highly damaged *M. helenor* and *M. achilles* display a reduction in the
325 typical flap-gliding flight observed in intact or less damaged individuals, progressively replaced
326 by strict flapping flight. As continuous flapping flight is more energetically-costly than gliding
327 flight (Dudley, 2002), the reduced gliding ability in strongly damaged individuals may result in
328 increased flight cost, ultimately impacting survival and/or reproductive abilities.

329 In previous studies investigating wing damage in insects, an increase in wingbeat frequency
330 (WBF) in damaged individuals has often been reported (Fernández et al., 2012; Hedenström et
331 al., 2001; Kingsolver, 1999; Muijres et al., 2017; Vance and Roberts, 2014), often associated with
332 increased metabolic costs. This kinematic adjustment allows maintaining sufficient lift in spite of
333 a reduced wing area (Altshuler et al., 2005; Dickinson et al., 1998). Higher WBF following wing
334 loss was measured during hovering flight in the butterfly *Pontia occidentalis* (Kingsolver, 1999)
335 and the moth *Manduca sexta* (Fernández et al., 2012). Damaged *Morpho* butterflies showed a
336 slight increase in WBF, at least during the forward flights studied here. Such increased frequency
337 mostly stem from the fewer gliding phases observed in damaged individuals, because the WBF
338 during flapping phases did not significantly increase in damages individuals as compared to intact
339 ones. In our experiment, *Morpho* butterflies thus do not modulate wingbeat frequency in response

340 to wing damage, but mostly limit gliding phases, switching from a flap-gliding flight to more
341 continuous flapping, with similar WBF. It has been shown that a reduced lift can be balanced by
342 an increase in either WBF or in stroke amplitude (Altshuler et al., 2005). *Morpho* may thus also
343 compensate wing damage by adjusting wing stroke amplitude rather than WBF. A more precise
344 comparison of kinematic parameters (such as wing stroke amplitude) of intact and damaged
345 individuals would thus be needed to test this hypothesis. Changes in WBF in response to wing
346 damage may also depend on the type of flight muscle involved. In asynchronous flyers (such as
347 flies or bees) a single nervous impulse triggers multiple contractions, allowing to reach high
348 wingbeat frequency (Dudley, 1991). In contrast, synchronous flyers (such as butterflies or
349 dragonflies) have a one to one correspondence between nervous impulses and muscle contraction
350 (Pringle, 1981). Physiological differences among insect species might impact their ability to
351 adjust WBF. Wing clipping in synchronous flyers indeed produces little effect on wingbeat
352 frequency (Roeder, 1951). The increase in wingbeat frequency associated with clipped wings was
353 found to be approximately 2 Hz in moths (Fernández et al., 2017), while an increase of 19 Hz and
354 23 Hz was measured in bees and flies respectively (Muijres et al., 2017; Vance and Roberts,
355 2014). Whether these changes in frequency reflect a behavioural adjustment or a passive
356 mechanical response is unknown. The capacity to increase wingbeat frequency may nonetheless
357 vary among insects, leading to different constraints on the evolution of wing shape and
358 toughness. *Morpho* butterflies showed a mean WBF of 5.9 ± 1.7 Hz, ranking them among the
359 lowest frequency found in insects (Sotavalta, 1947). Such a low WBF is expected given that their
360 flight is composed of frequent alternations between flapping and gliding phases.

361
362 **The relative importance of different wing parts for flight**
363 How the distribution of missing area over the wings impacts flight behaviour has been rarely
364 tested, and allows pinpointing the implications of different wing parts in flight performance. Our
365 results clearly point at an unequal impact of fore- and hindwings damages on *Morpho* flight:
366 damage on forewings affected more strongly flight performance than that on hindwings. The loss
367 of forewing area significantly reduced flight speed and the proportion of gliding flight.
368 Experimental wing manipulations have shown that complete removal of the forewings makes
369 butterflies flightless, while they can still fly without the hindwings (Jantzen and Eisner, 2008).
370 Interestingly, we found that damages specifically located at the tip of the forewings – altering the

371 shape of the leading edge – most strongly impaired flight speed and gliding ability of *Morpho*
372 butterflies, probably because the leading edge of the wing is strongly involved in lift generation:
373 during flight, the incoming air flow separates precisely as it crosses the leading edge, producing a
374 vortex (termed leading edge vortex) that creates a suction force resulting in lift enhancement
375 (Ellington et al., 1996; Sane, 2003). Butterflies with deteriorated leading edge face a substantial
376 reduction in lift generation.

377 While the most anteriorly located wing damages had severe consequences on flight, the loss of
378 other wing parts seemed to be relatively harmless: expansion of damages located along the
379 forewing margin had no detectable effect on flight.

380 Damage on the hindwings showed only limited effect on flight parameters: the clearest impact
381 was on flight height that was reduced in damaged individuals, pointing at a possible role for the
382 hindwings in upwards flight. Such an effect would deserve to be tested in a more controlled
383 experiment. In particular, it would be interesting to investigate the role of hindwings for upward
384 escape from predators, and especially during take-off. This could have important consequences
385 on hindwing shape evolution. Jantzen and Eisner (2008) showed that hindwings removal in
386 butterflies was associated with significant reduction in linear and turning accelerations, limiting
387 performances in zig-zag, erratic flight, and therefore putatively decreasing the capacity to escape
388 flying predators. Here we did not find such effect, possibly because the distribution of damages
389 over the four wings varied greatly between individuals, limiting our statistical power.

390

391 **Contrasted behavioural compensation between species**

392 *M. helenor* and *M. achilles* are two sister species showing extreme phenotypic similarity and
393 occupying the same microhabitat (Blandin, 1988; Chazot et al., 2016). Nevertheless, our results
394 show that behavioural changes triggered by wing damage differed between these two *Morpho*
395 species. While wing area loss resulted in decrease in flight speed and in gliding proportion for
396 both species, flight speed decreased significantly more in *M. helenor* as compared to *M. achilles*.
397 In contrast, the gliding ability of *M. achilles* was more impaired by wing damage relative to *M.*
398 *helenor*. However, no difference in any flight parameters was found between species when
399 considering only intact individuals, and similar damage proportions were observed in both
400 species. This behavioural difference may stem from subtle differences in the location of lost areas
401 among damaged *M. helenor* and *M. achilles*, differently impacting their flight. Nevertheless, by

402 constraining butterflies to fly with severely damaged wings, we may also have revealed
403 differences in flight behaviour or morphology between species (such as muscles mass, position
404 and power), that would otherwise have remained undetectable (i.e. in less challenging
405 conditions). Challenging conditions eliciting extreme performance have indeed been shown to
406 reveal the consequences of morphological or physiological variations more readily than
407 favourable conditions (Losos et al., 2002; Wainwright and Reilly, 1994). This apparent difference
408 between *M. achilles* and *M. helenor* in their behavioural ability to compensate wing damage
409 points at the need to consider the interactions between wing shape and other behavioural and
410 morphological traits when investigating the evolution of wing shape across butterfly species.

411
412 **Predictions on the evolution of butterflies fore- and hindwings drawn from the effect of natural**
413 **damage on flight capacities.**

414 Our results highlight that impaired flight performances (and possible behavioural compensations)
415 do not only depend on the extent of damage, but also on their location over the wings. The crucial
416 role of the leading edge in flight for instance might generate a strong selection on its toughness.
417 The evolution of a close proximity and even fusion of several veins in the anterior part of insect
418 wings might also stem from such selection on wing toughness (Dudley, 2002; Rees, 1975).
419 Deteriorated leading edge was indeed rarely observed in our sample of naturally damaged
420 individuals, and only found in captive individuals experiencing frequent collisions with the rough
421 cage walls. These extreme damages contrast with those observed in wild-caught individuals, such
422 as scattered tearing along the wing margin, with limited impact on flight performance. The
423 damages observed in wild-caught individuals likely illustrate a range of wing shape alterations
424 with limited impact on survival. Such harmless consequences of wing margin damages may
425 explain the evolution of eyespots along the wing margin in some butterfly species (e.g. in
426 *Bicyclus anynana*), shown to deflect predators attacks away from vital body parts (Lyytinen et al.,
427 2003; Stevens, 2005). Further field studies quantifying natural wing damages in butterflies should
428 assess the frequency of scattered margins in the wild, particularly in species displaying peripheral
429 eyespots. Experimental manipulations of wing shape are still required to rigorously test the effect
430 of quantitatively similar, but spatially different wing loss, to identify the selection regimes
431 affecting the various parts of the wing and thus altering wing shape evolution.

432 Because alterations of forewings shape have a much more severe impact on flight

433 performances, forewing shape may be under stronger stabilizing selection than hindwing shape.
434 Strauss (1990) found that wing shape variation in Heliconiinae and Ithomiinae butterflies
435 increased from the anterior part of the forewing to the posterior part of the hindwing. Such an
436 increasing shape variability and conversely a decreasing density of veins along the chordwise
437 wing section may reflect an antero-posterior decrease in aerodynamic constrains. Lepidoptera
438 hindwings frequently show large shape variations between species, such as the presence of
439 scalloped edges or expanded tails (Robbins, 1981; Rubin et al., 2018), contrasting with the
440 generally subtler variation in forewing shape. Hindwing tails that closely resemble butterfly's
441 head in some Lycaenids species are thought to deflect predators attacks (López-Palafox and
442 Cordero, 2017; Robbins, 1981). Similarly, tails in moths were recently shown to have a deflecting
443 role against bat attacks (Barber et al., 2015; Rubin et al., 2018). The evolution of marked
444 hindwing extensions in response to predation suggests that a large shape variation may occur on
445 butterfly hindwings with limited effects on flight performance. Aerodynamic constraints on
446 hindwings may then be slighter than those acting on forewings, limiting the deleterious impact of
447 evolution of hindwing variations on flight performance.

448 Altogether, by studying wing shape variations induced by natural damages, our work suggest
449 that contrasted selective regimes may act on different wing parts of *Morpho* butterflies,
450 highlighting wing areas under stabilizing and relaxed selection. Ascertaining the variation in
451 aerodynamic constraints within and between insect wings may then provide important insight on
452 the evolution of wing morphologies. A better understanding of these constraints should stem from
453 further experimental studies generating a large diversity of wing damages.

454

455 **Acknowledgements**

456 The authors would like to thank the Peruvian authorities, and in particular SERFOR (permit: 002-
457 2015-SERFOR-DGGSPFF) for providing the necessary research permits. We thank Ronald Mori-
458 Pezo, Corentin Clerc, César, Jay and Bruno Ramirez for help with the sampling of butterflies. We
459 are grateful to Tyson Hedrick for his advices on the three-dimensional videography method. We
460 thanks two anonymous reviewers for helpful comments on the first draft.

461

462 **Competing interests**

463 The authors declare no competing of financial interests.

464

465 **Author contributions**

466 C.L.R., V.D. and V.L. designed the experiment and participated to the field sampling. C.L.R.
467 performed the filming, the three-dimensional reconstruction, the photographs acquisition and the
468 statistical analysis. V.D. and R.C. designed the geometric morphometrics analysis. C.L.R., V.D.
469 and V.L. wrote the manuscript.

470

471 **Funding**

472 This work was funded by the Université Paris Descartes, the Ecole Doctoral FIRE – Programme
473 Bettencourt, and the Labex BCDiv to C.L.R., and the Emergence program of Paris city council to
474 V.L.

475

476 **References**

477 **Adams, D. C. and Otárola-Castillo, E.** (2013). geomorph: an R package for the
478 collection and analysis of geometric morphometric shape data. *Methods in Ecology and Evolution*
479 **4**, 393-399.

480 **Adams, D. C., Rohlf, F. J. and Slice, D. E.** (2004). Geometric morphometrics: ten years
481 of progress following the ‘revolution’. *Italian Journal of Zoology* **71**, 5-16.

482 **Alcock, J.** (1996). Male size and survival: the effects of male combat and bird predation
483 in Dawson’s burrowing bees, *Amegilladawsoni*. *Ecological entomology* **21**, 309-316.

484 **Altizer, S. and Davis, A. K.** (2010). Populations of monarch butterflies with different
485 migratory behaviors show divergence in wing morphology. *Evolution: International Journal of*
486 *Organic Evolution* **64**, 1018-1028.

487 **Altshuler, D. L., Dickson, W. B., Vance, J. T., Roberts, S. P. and Dickinson, M. H.**
488 (2005). Short-amplitude high-frequency wing strokes determine the aerodynamics of honeybee
489 flight. *Proceedings of the National Academy of Sciences* **102**, 18213-18218.

490 **Ancel, A. O., Eastwood, R., Vogt, D., Ithier, C., Smith, M., Wood, R. and Kovač, M.**
491 (2017). Aerodynamic evaluation of wing shape and wing orientation in four butterfly species
492 using numerical simulations and a low-speed wind tunnel, and its implications for the design of
493 flying micro-robots. *Interface Focus* **7**, 20160087.

494 **Arnold, S. J.** (1983). Morphology, performance and fitness. *American zoologist* **23**, 347-
495 361.

496 **Barber, J. R., Leavell, B. C., Keener, A. L., Breinholt, J. W., Chadwell, B. A.,**
497 **McClure, C. J., Hill, G. M. and Kawahara, A. Y.** (2015). Moth tails divert bat attack: evolution
498 of acoustic deflection. *Proceedings of the National Academy of Sciences* **112**, 2812-2816.

499 **Berwaerts, K., Aerts, P. and Van Dyck, H.** (2006). On the sex-specific mechanisms of
500 butterfly flight: flight performance relative to flight morphology, wing kinematics, and sex in
501 *Pararge aegeria*. *Biological Journal of the Linnean Society* **89**, 675-687.

502 **Blandin, P.** (1988). The Genus *Morpho* (Lepidoptera, Nymphalidae): Sciences Nat.

503 **Bonhomme, V., Picq, S., Gaucherel, C. and Claude, J.** (2014). Momocs: outline
504 analysis using R. *Journal of Statistical Software* **56**, 1-24.

505 **Bookstein, F. L.** (1997). Morphometric tools for landmark data: geometry and biology:
506 Cambridge University Press, Cambridge.

507 **Breuker, C. J., Gibbs, M., Van Dongen, S., Merckx, T. and Van Dyck, H.** (2010). The
508 use of geometric morphometrics in studying butterfly wings in an evolutionary ecological
509 context. In *Morphometrics for Nonmorphometricians*, pp. 271-287: Springer.

510 **Butterworth, S.** (1930). On the theory of filter amplifiers. *Wireless Engineer* **7**, 536-541.

511 **Carpenter, D., GD Hale.** (1942). The Relative Frequency of Beak-marks on Butterflies
512 of Different/Edibility to Birds. In *Proceedings of the Zoological Society of London*, vol. 111, pp.
513 223-231: Wiley Online Library.

514 **Cartar, R. V.** (1992). Morphological senescence and longevity: an experiment relating
515 wing wear and life span in foraging wild bumble bees. *Journal of Animal Ecology* **61**, 225-231.

516 **Carvalho, M., Peixoto, P. and Benson, W.** (2016). Territorial clashes in the Neotropical
517 butterfly *Actinote pellenea* (Acraeinae): do disputes differ when contests get physical?
518 *Behavioral ecology and sociobiology* **70**, 199-207.

519 **Chai, P. and Srygley, R. B.** (1990). Predation and the flight, morphology, and
520 temperature of neotropical rain-forest butterflies. *The American Naturalist* **135**, 748-765.

521 **Chazot, N., Panara, S., Zilbermann, N., Blandin, P., Le Poul, Y., Cornette, R., Elias,
522 M. and Debat, V.** (2016). Morpho morphometrics: Shared ancestry and selection drive the
523 evolution of wing size and shape in *Morpho* butterflies. *Evolution* **70**, 181-194.

524 **Combes, S., Crall, J. and Mukherjee, S.** (2010). Dynamics of animal movement in an
525 ecological context: dragonfly wing damage reduces flight performance and predation success.
526 *Biology letters* **6**, 426-429.

527 **DeVries, P., Penz, C. M. and Hill, R. I.** (2010). Vertical distribution, flight behaviour and
528 evolution of wing morphology in *Morpho* butterflies. *Journal of Animal Ecology* **79**, 1077-1085.

529 **Dickinson, M. H., Lehmann, F.-O. and Chan, W. P.** (1998). The control of mechanical
530 power in insect flight. *American zoologist* **38**, 718-728.

531 **Dockx, C.** (2007). Directional and stabilizing selection on wing size and shape in migrant
532 and resident monarch butterflies, *Danaus plexippus* (L.), in Cuba. *Biological Journal of the
533 Linnean Society* **92**, 605-616.

534 **Dudley, R.** (1991). Comparative biomechanics and the evolutionary diversification of
535 flying insect morphology. In *The Unity of Evolutionary Biology* (ed. E. C. Dudley), pp. 503-514.
536 Portland, OR: Dioscorides Press.

537 **Dudley, R.** (2002). The biomechanics of insect flight: form, function, evolution.
538 Princeton: Princeton University Press.

539 **Edmunds, M.** (1974). Significance of beak marks on butterfly wings. *Oikos, Acta Oecol
540 Scand* **42**, 467-480.

541 **Ellington, C.** (1984). The aerodynamics of insect flight. II. Morphological parameters.
542 *Phil. Trans. R. Soc. Lond. B* **305**, 17-40.

543 **Ellington, C. P., Van Den Berg, C., Willmott, A. P. and Thomas, A. L.** (1996).
544 Leading-edge vortices in insect flight. *Nature* **384**, 626.

545 **Escoufier, Y.** (1973). Le traitement des variables vectorielles. *Biometrics* **29**, 751-760.

546 **Fernández, M. J., Driver, M. E. and Hedrick, T. L.** (2017). Asymmetry costs: effects of
547 wing damage on hovering flight performance in the hawkmoth *Manduca sexta*. *Journal of
548 Experimental Biology* **220**, 3649-3638.

549 **Fernández, M. J., Springthorpe, D. and Hedrick, T. L.** (2012). Neuromuscular and
550 biomechanical compensation for wing asymmetry in insect hovering flight. *Journal of*
551 *Experimental Biology* **215**, 3631-3638.

552 **Foster, D. J. and Cartar, R. V.** (2011). What causes wing wear in foraging bumble bees?
553 *Journal of Experimental Biology* **214**, 1896-1901.

554 **French, J. P.** (2017). autoimage: Multiple Heat Maps for Projected Coordinates. *The R*
555 *journal* **9**, 284.

556 **Gunz, P. and Mitteroecker, P.** (2013). Semilandmarks: a method for quantifying curves
557 and surfaces. *Hystrix, the Italian Journal of Mammalogy* **24**(1), 103-109.

558 **Haas, C. and Cartar, R.** (2008). Robust flight performance of bumble bees with
559 artificially induced wing wear. *Canadian Journal of Zoology* **86**, 668-675.

560 **Hall, J. P. and Willmott, K. R.** (2000). Patterns of feeding behaviour in adult male
561 riodinid butterflies and their relationship to morphology and ecology. *Biological Journal of the*
562 *Linnean Society* **69**, 1-23.

563 **Hartley, R. I. and Sturm, P.** (1995). Triangulation. In *International Conference on*
564 *Computer Analysis of Images and Patterns*, pp. 190-197: Springer.

565 **Hedenström, A., Ellington, C. and Wolf, T.** (2001). Wing wear, aerodynamics and flight
566 energetics in bumblebees (*Bombus terrestris*): an experimental study. *Functional Ecology* **15**,
567 417-422.

568 **Hedrick, T. L.** (2008). Software techniques for two-and three-dimensional kinematic
569 measurements of biological and biomimetic systems. *Bioinspiration & biomimetics* **3**, 034001.

570 **Higginson, A. and Barnard, C.** (2004). Accumulating wing damage affects foraging
571 decisions in honeybees (*Apis mellifera* L.). *Ecological Entomology* **29**, 52-59.

572 **Jackson, B. E., Evangelista, D. J., Ray, D. D. and Hedrick, T. L.** (2016). 3D for the
573 people: multi-camera motion capture in the field with consumer-grade cameras and open source
574 software. *Biology open* **5**, 1334-1342.

575 **Jantzen, B. and Eisner, T.** (2008). Hindwings are unnecessary for flight but essential for
576 execution of normal evasive flight in Lepidoptera. *Proceedings of the National Academy of*
577 *Sciences* **105**, 16636-16640.

578 **Johansson, F., Söderquist, M. and Bokma, F.** (2009). Insect wing shape evolution:
579 independent effects of migratory and mate guarding flight on dragonfly wings. *Biological*
580 *Journal of the Linnean Society* **97**, 362-372.

581 **KaewTraKulPong, P. and Bowden, R.** (2002). An improved adaptive background
582 mixture model for real-time tracking with shadow detection. In *Video-based surveillance systems*,
583 pp. 135-144: Springer.

584 **Kingsolver, J. G.** (1999). Experimental analyses of wing size, flight, and survival in the
585 western white butterfly. *Evolution* **53**, 1479-1490.

586 **Klingenberg, C. P.** (2009). Morphometric integration and modularity in configurations of
587 landmarks: tools for evaluating a priori hypotheses. *Evolution & development* **11**, 405-421.

588 **Kwon, Y.** (1998). Kwon3D: Camera Calibration - DLT Method.
589 <http://www.kwon3d.com/theory/dlt/dlt.html>.

590 **Le Roy, C., Debat, V. and Llaurens, V.** (2019). Adaptive evolution of butterfly wing
591 shape: from morphology to behaviour. *Biological Reviews*. (In press)

592 **López-Palafox, T. G. and Cordero, C. R.** (2017). Two-headed butterfly vs. mantis: do
593 false antennae matter? *PeerJ* **5**, e3493.

594 **Losos, J. B., Creer, D. A. and Schulte II, J. A.** (2002). Cautionary comments on the
595 measurement of maximum locomotor capabilities. *Journal of Zoology* **258**, 57-61.

596 **Lyytinen, A., Brakefield, P. M. and Mappes, J.** (2003). Significance of butterfly
597 eyespots as an anti-predator device in ground-based and aerial attacks. *Oikos* **100**, 373-379.

598 **Mountcastle, A. M. and Combes, S. A.** (2014). Biomechanical strategies for mitigating
599 collision damage in insect wings: structural design versus embedded elastic materials. *Journal of*
600 *Experimental Biology* **217**, 1108-1115.

601 **Muijres, F. T., Iwasaki, N. A., Elzinga, M. J., Melis, J. M. and Dickinson, M. H.**
602 (2017). Flies compensate for unilateral wing damage through modular adjustments of wing and
603 body kinematics. *Interface Focus* **7**, 20160103.

604 **Norberg, U. M. and Rayner, J. M.** (1987). Ecological morphology and flight in bats
605 (Mammalia; Chiroptera): wing adaptations, flight performance, foraging strategy and
606 echolocation. *Phil. Trans. R. Soc. Lond. B* **316**, 335-427.

607 **Outomuro, D. and Johansson, F.** (2015). Bird predation selects for wing shape and
608 coloration in a damselfly. *Journal of evolutionary biology* **28**, 791-799.

609 **Pau, G., Fuchs, F., Sklyar, O., Boutros, M. and Huber, W.** (2010). EBImage—an R
610 package for image processing with applications to cellular phenotypes. *Bioinformatics* **26**, 979-
611 981.

612 **Pringle, J.** (1981). The Bidder Lecture, 1980 the evolution of fibrillar muscle in insects.
613 *Journal of Experimental Biology* **94**, 1-14.

614 **Rayner, J. M.** (1988). Form and function in avian flight. In *Current ornithology* **5**, 1-66.

615 **Rees, C. J.** (1975). Form and function in corrugated insect wings. *Nature* **256**, 200.

616 **Robbins, R. K.** (1981). The "false head" hypothesis: predation and wing pattern variation
617 of lycaenid butterflies. *The American Naturalist* **118**, 770-775.

618 **Roeder, K. D.** (1951). Movements of the thorax and potential changes in the thoracic
619 muscles of insects during flight. *The Biological Bulletin* **100**, 95-106.

620 **Rohlf, F. J.** (2015). The tps series of software. *Hystrix* **26**, 1-4.

621 **Rohlf, F. J. and Corti, M.** (2000). Use of two-block partial least-squares to study
622 covariation in shape. *Systematic Biology* **49**, 740-753.

623 **Rohlf, F. J. and Slice, D.** (1990). Extensions of the Procrustes method for the optimal
624 superimposition of landmarks. *Systematic Biology* **39**, 40-59.

625 **Rubin, J. J., Hamilton, C. A., McClure, C. J., Chadwell, B. A., Kawahara, A. Y. and**
626 **Barber, J. R.** (2018). The evolution of anti-bat sensory illusions in moths. *Science Advances* **4**, 1-
627 10.

628 **Sane, S. P.** (2003). The aerodynamics of insect flight. *Journal of Experimental Biology*
629 **206**, 4191-4208.

630 **Scott, J. A.** (1974). Mate-locating behavior of butterflies. *American Midland Naturalist*
631 **91**, 103-117.

632 **Shapiro, A. M.** (1974). Beak-mark frequency as an index of seasonal predation intensity
633 on common butterflies. *The American Naturalist* **108**, 229-232.

634 **Sotavalta, O.** (1947). The Flight-tone (wing-stroke Frequency) of Insects. *Acta entomol.*
635 *fennica.* **4**, 1-117.

636 **Stevens, M.** (2005). The role of eyespots as anti-predator mechanisms, principally
637 demonstrated in the Lepidoptera. *Biological Reviews* **80**, 573-588.

638 **Strauss, R. E.** (1990). Patterns of quantitative variation in lepidopteran wing
639 morphology: the convergent groups Heliconiinae and Ithomiinae (Papilionoidea: Nymphalidae).
640 *Evolution* **44**, 86-103.

641 **Team, R. C.** (2013). R: A language and environment for statistical computing.

642 **Theriault, D. H., Fuller, N. W., Jackson, B. E., Bluhm, E., Evangelista, D., Wu, Z.,**

643 **Betke, M. and Hedrick, T. L.** (2014). A protocol and calibration method for accurate multi-
644 camera field videography. *Journal of Experimental Biology* **217**, 1843-1848.
645 **Vance, J. T. and Roberts, S. P.** (2014). The effects of artificial wing wear on the flight
646 capacity of the honey bee *Apis mellifera*. *Journal of insect physiology* **65**, 27-36.
647 **Wainwright, P. C. and Reilly, S. M.** (1994). *Ecological morphology: integrative*
648 *organismal biology*. Chicago: University of Chicago Press.
649 **Wickman, P. O.** (1992). Sexual selection and butterfly design—a comparative study.
650 *Evolution* **46**, 1525-1536.
651 **Wootton, R. J.** (1992). Functional morphology of insect wings. *Annual review of*
652 *entomology* **37**, 113-140.
653 **Zhong, M., Hill, G. M., Gomez, J. P., Plotkin, D., Barber, J. R. and Kawahara, A. Y.**
654 (2016). Quantifying wing shape and size of saturniid moths with geometric morphometrics. *The*
655 *Journal of the Lepidopterists' Society* **70**, 99-107.

656
657
658
659 **Figure Legends**

660
661
662 **Tab. 1.** Correlation coefficients between flight parameters and the flight component of PLS 1 and
663 PLS2.

664
665 **Fig. 1.** Three-dimensional trajectory of a *Morpho* butterfly. Upward and downward directed
666 triangles are drawn when the butterfly wings are at the uppermost and lowermost most positions
667 during the upstroke and downstroke respectively. Based on wing stroke positions along the
668 trajectory, gliding and flapping phases are distinguished. Duration of the shown trajectory is 1.7
669 seconds.

670
671 **Fig. 2.** Heat map describing variation in spatial location of wing damage. Left: individuals kept in
672 mesh-cage for three days. Right: naturally damaged individuals. Left and right wings are pooled
673 together for each pair of wings. Most frequent damages are in dark red.

674
675 **Tab. 1.** Correlation coefficients between flight parameters and the flight component of PLS 1 and
676 PLS2.

677
678 **Fig. 3.** PLS analysis showing covariation between wing damage and flight. Covariation detected
679 on the first (A) and second (B) PLS vectors are shown. Shades of grey indicate the number of
680 wings damaged at a threshold of >5% of wing area loss. Some of the specimen's wing shape are
681 shown to facilitate visual interpretation. See Table 1 for variation in flight parameters along the y
682 axis

683
684 **Fig. 4.** Effect of forewing area loss on flight speed and gliding proportion. Forewing area loss
685 have a negative effect on flight speed and gliding proportion in both studied species. Despite this
686 effect, *Morpho achilles* and *M. helenor* can be distinguished by their flight behaviour: *M. achilles*
687 shows higher flight speed relative to *M. helenor*, but *M. helenor* tends to glide more than *M.*
688 *achilles*. R² values shown correspond to the global regression, both species pooled.

689
690
691
692
693
694
695

Fig. 5. Effect of different damage distribution on flight speed. Relationship between flight speed and PC1 (A), and PC2 (B), each carrying different types of forewings shape alteration. While damages located along the margins (extreme values on PC1) have no effect on flight speed, those mostly affecting the wing tip (extreme values on PC2) reduce flight speed. Variation in damage is shown with heat maps generated on three groups of 21 individuals along the PCs axes.

Figure 1

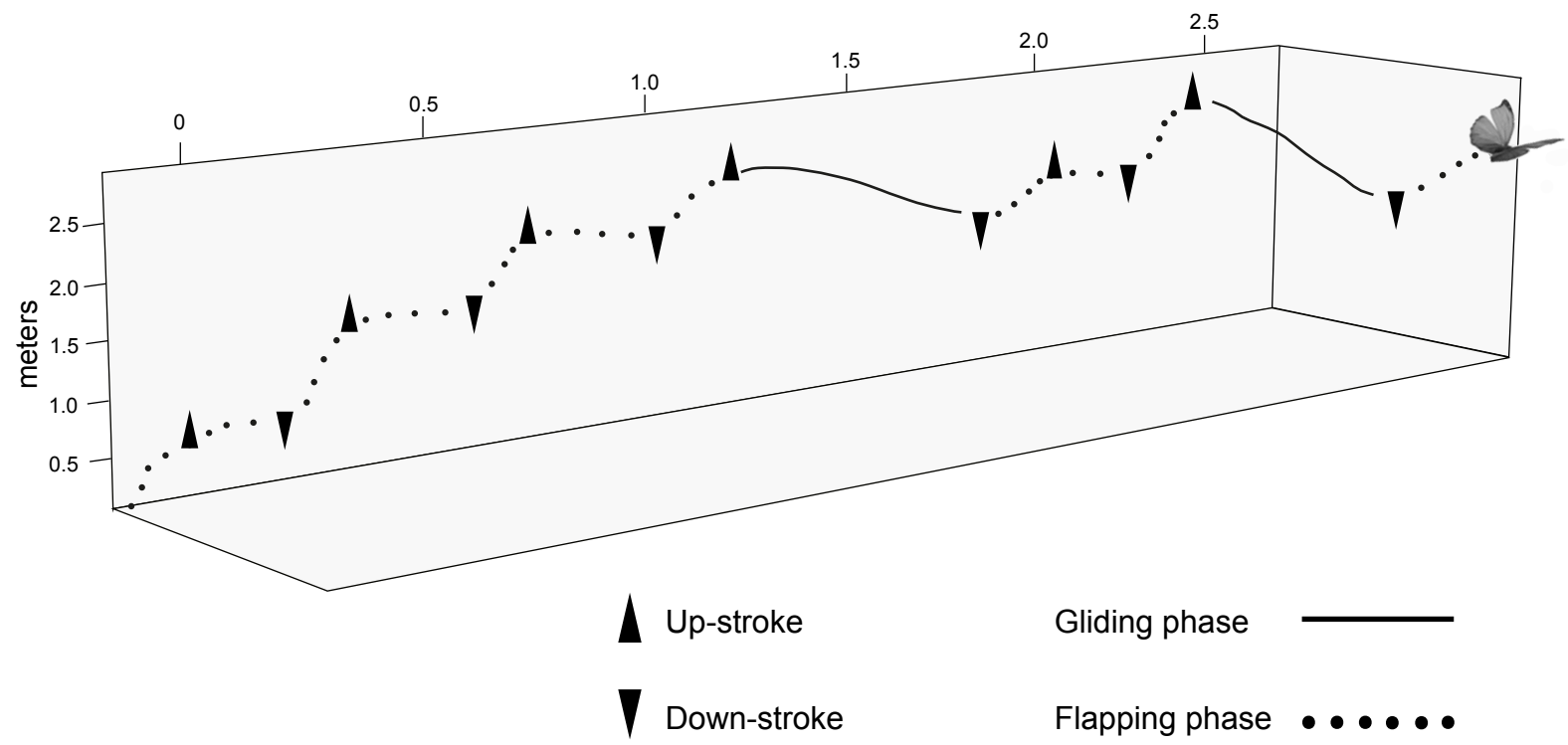
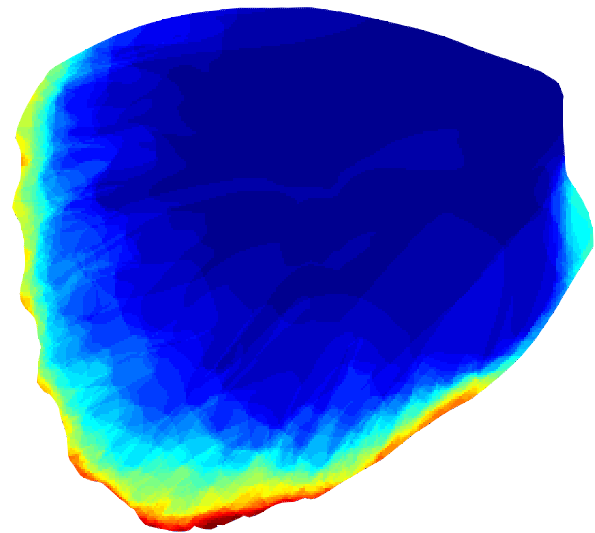
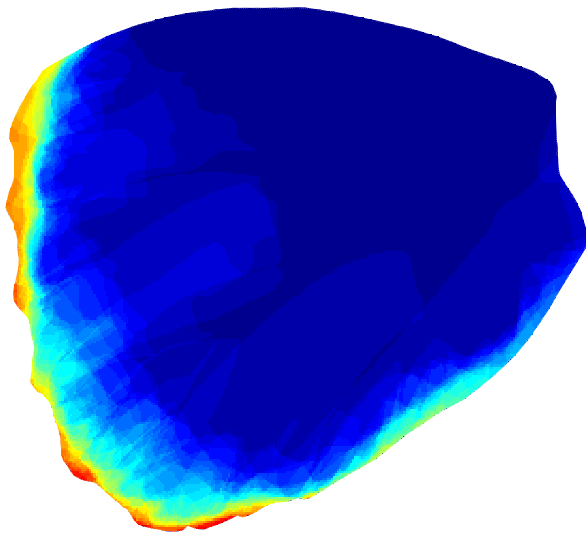
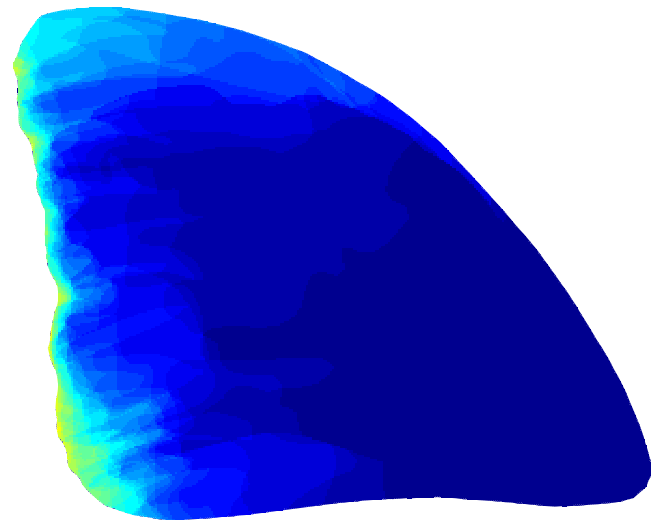
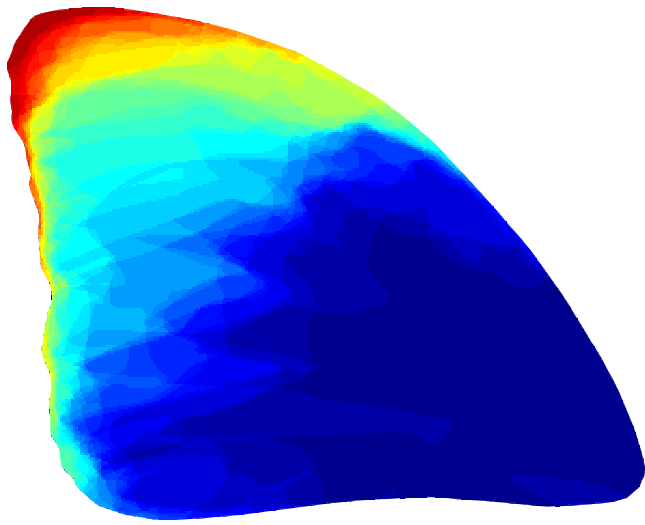


Figure 2

Cage
N = 25 ind.

Nature
N = 38 ind.




1 ind.  21 ind.

Figure 3A

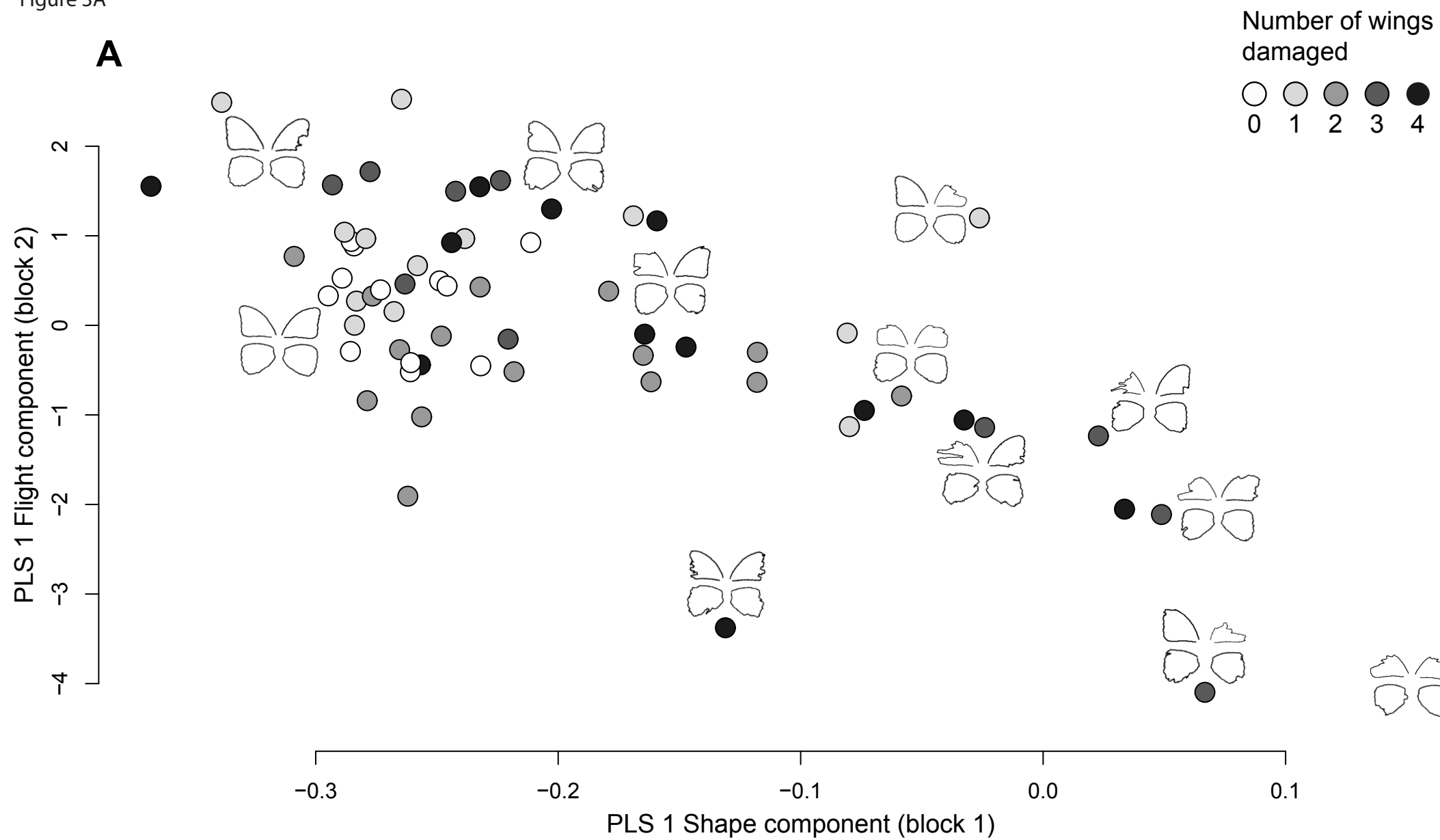
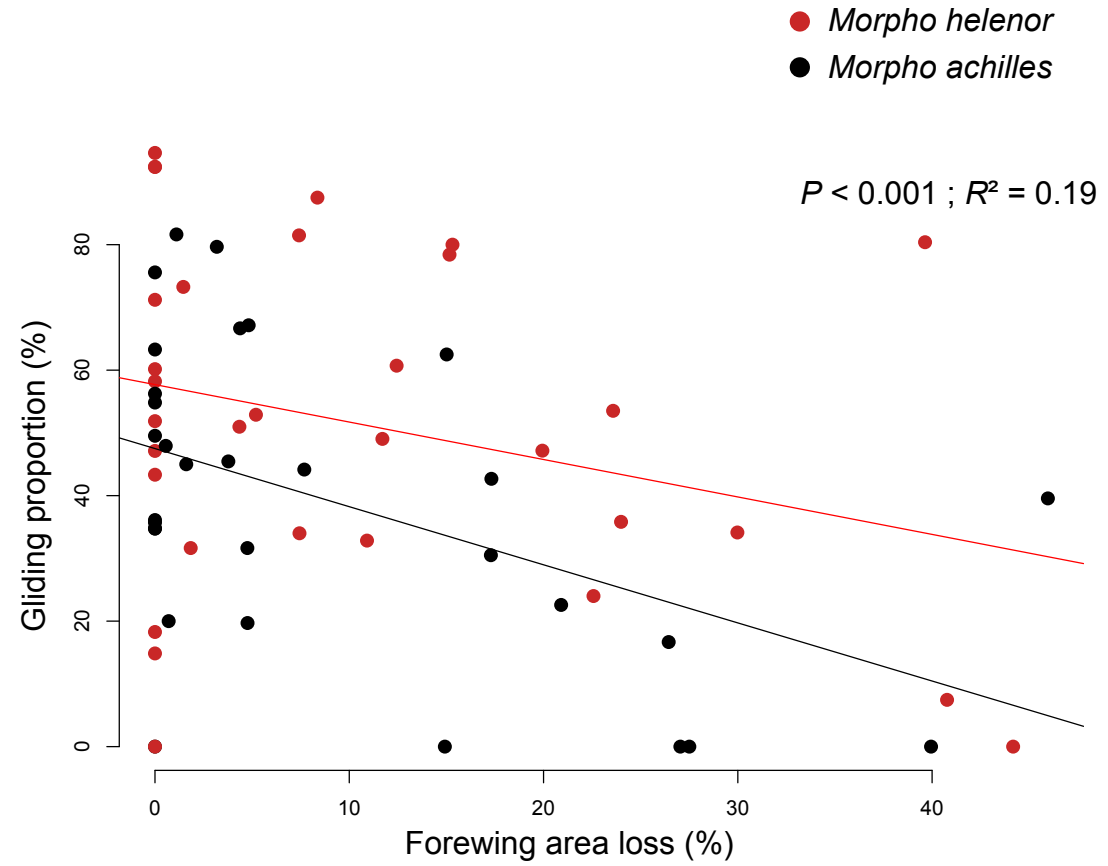
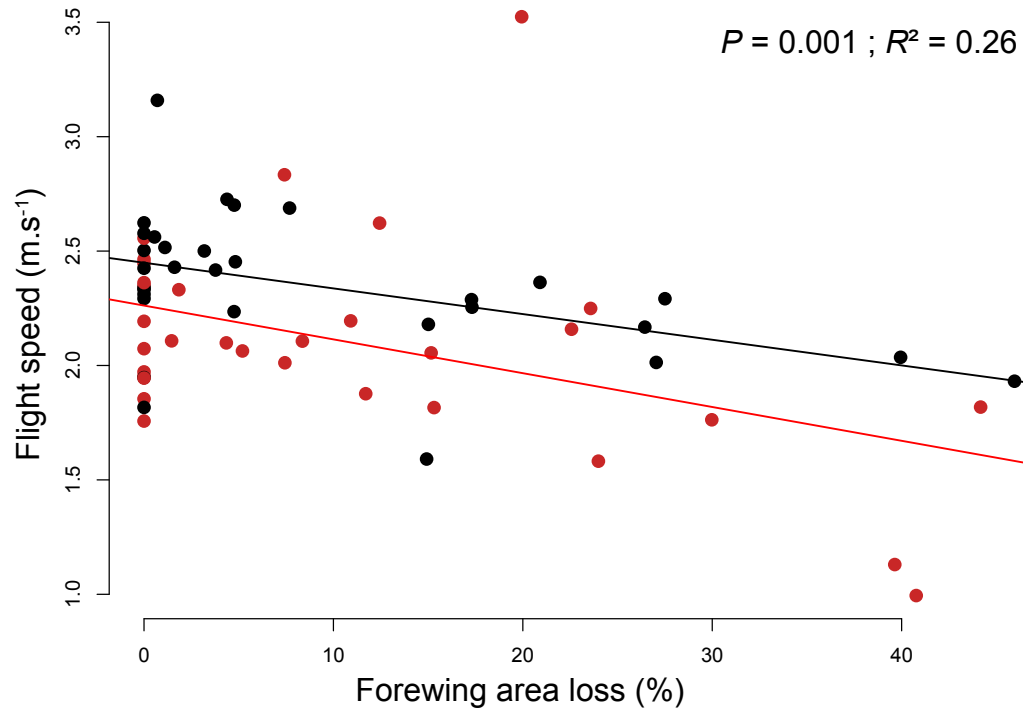


Figure 4



A Figure 5A

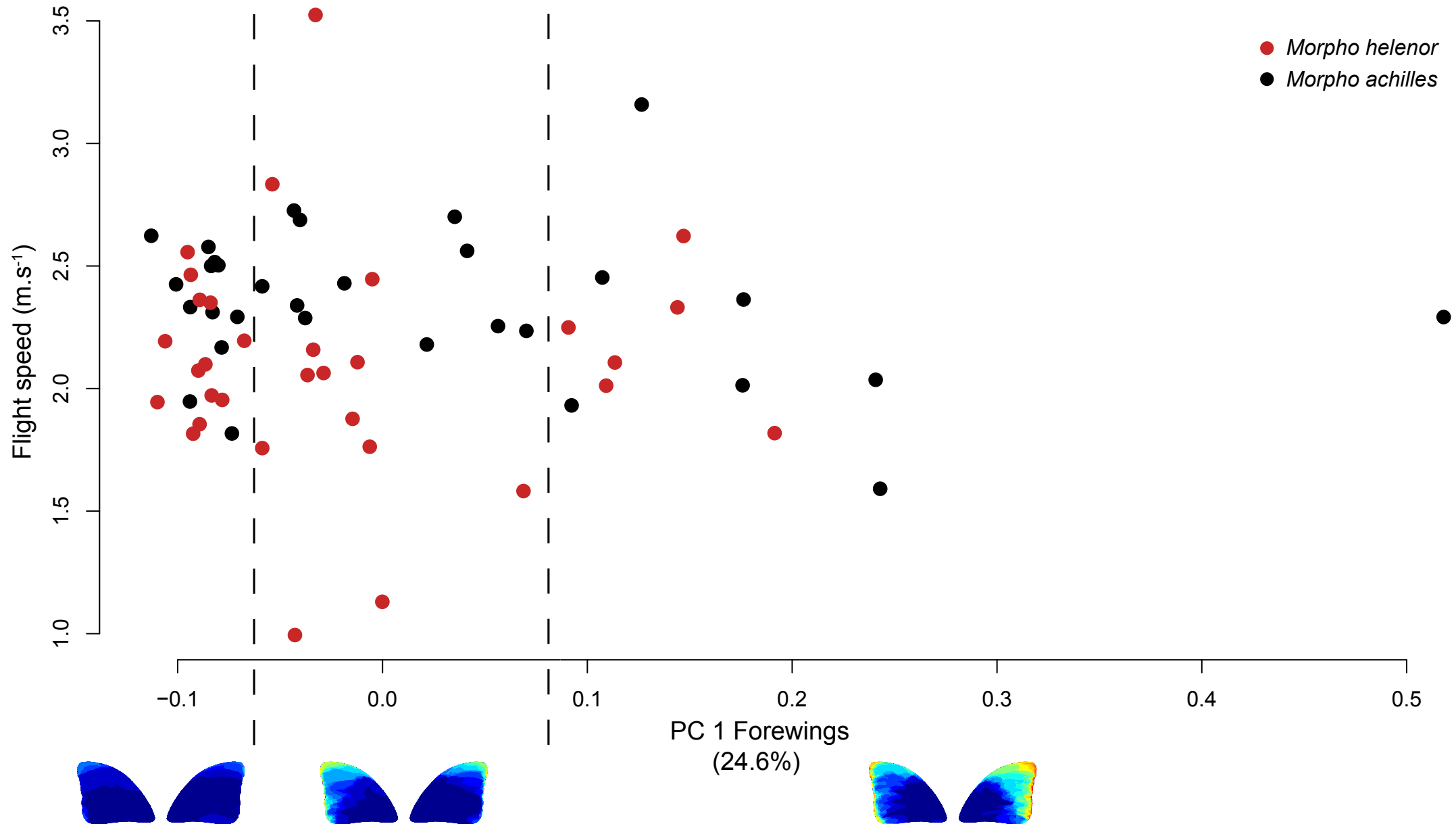
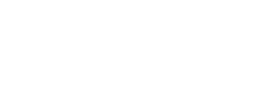
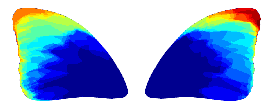
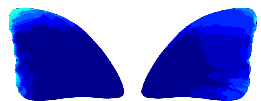
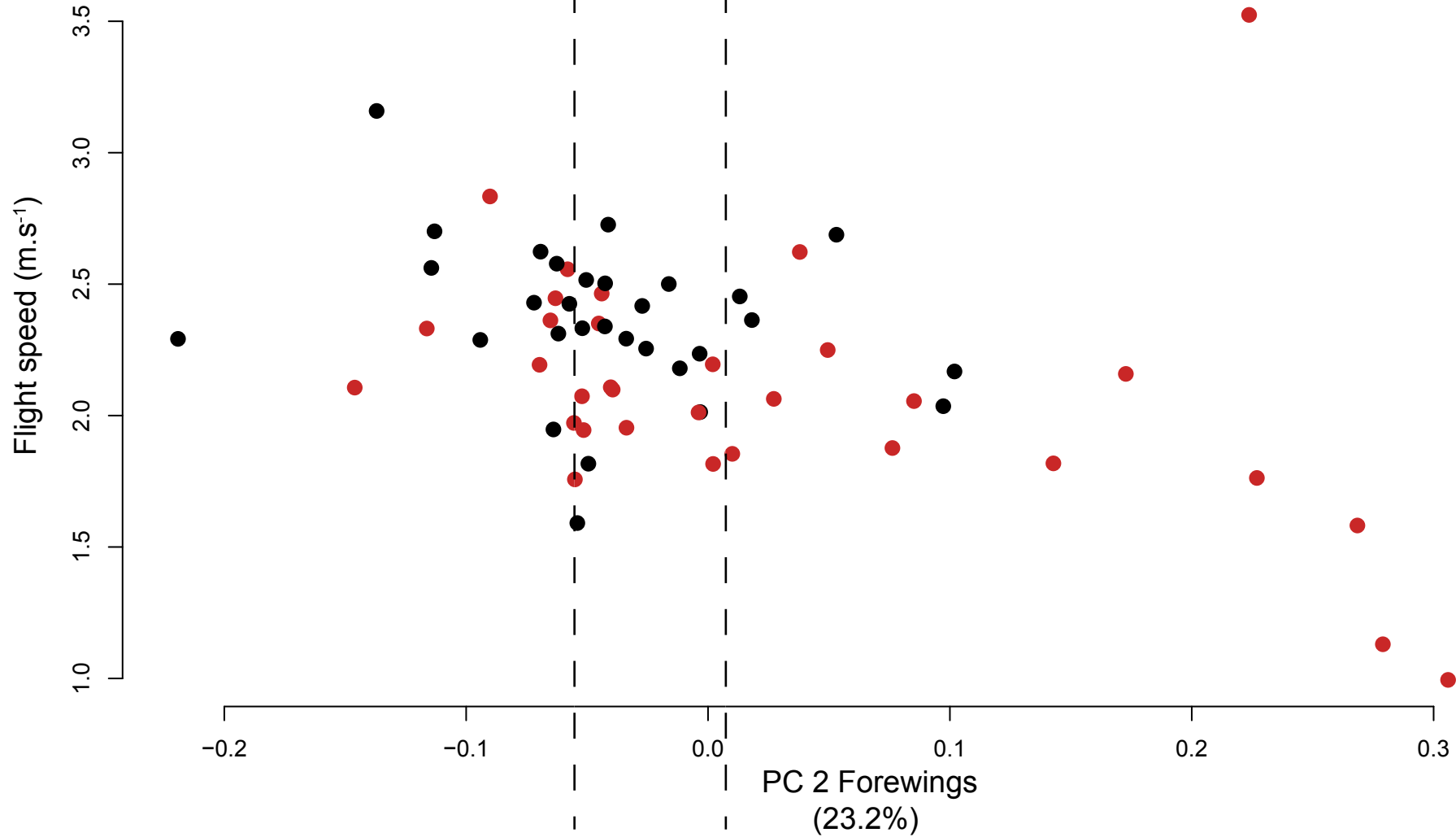


Figure 5B

B



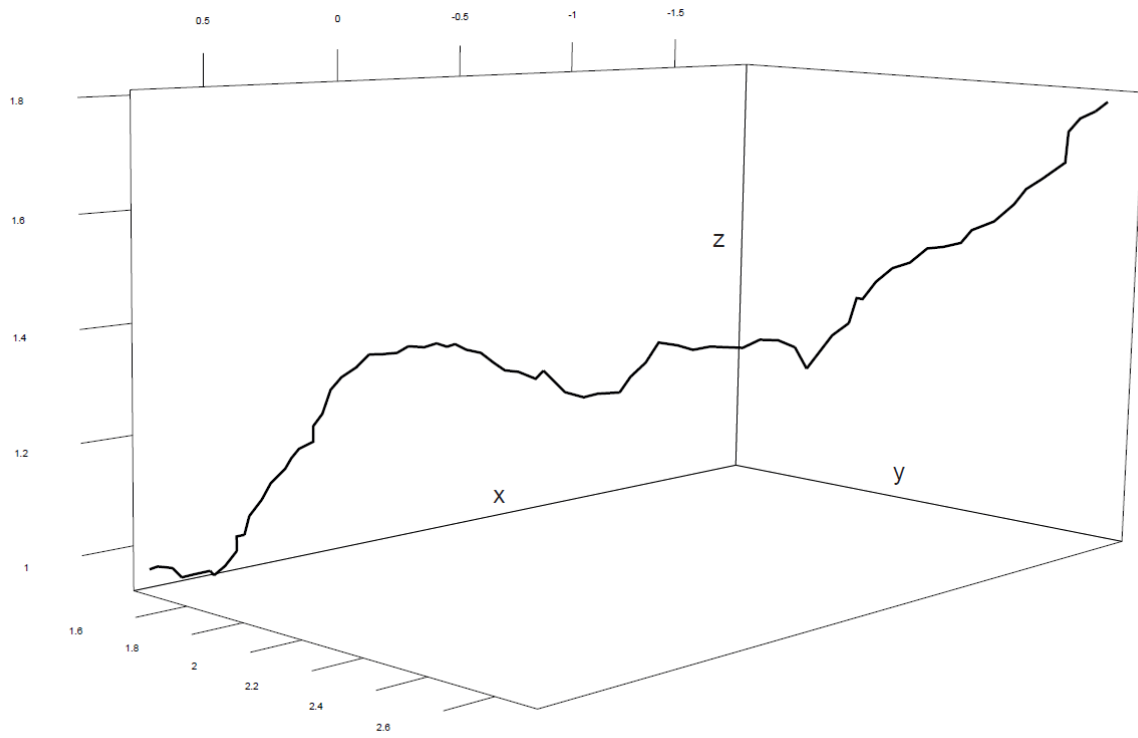
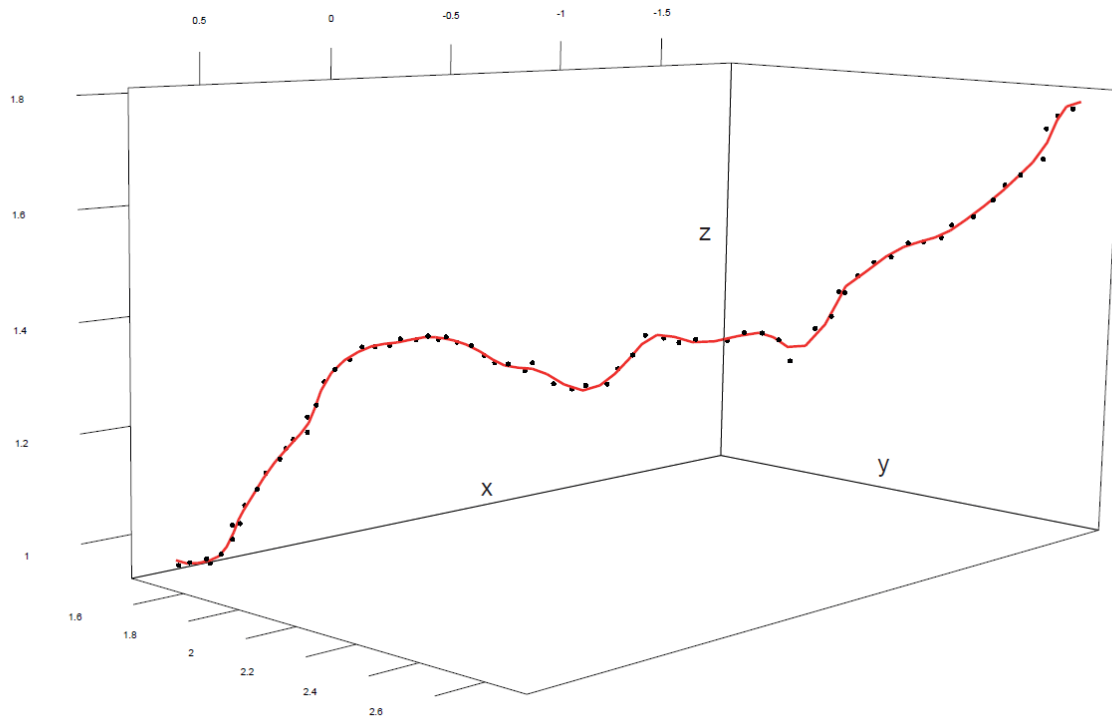
A**B**

Figure S1. Trajectory smoothing using low pass Butterworth filter. A raw flight trajectory of a single individual (A), and its corresponding smoothed trajectory shown in red (B).

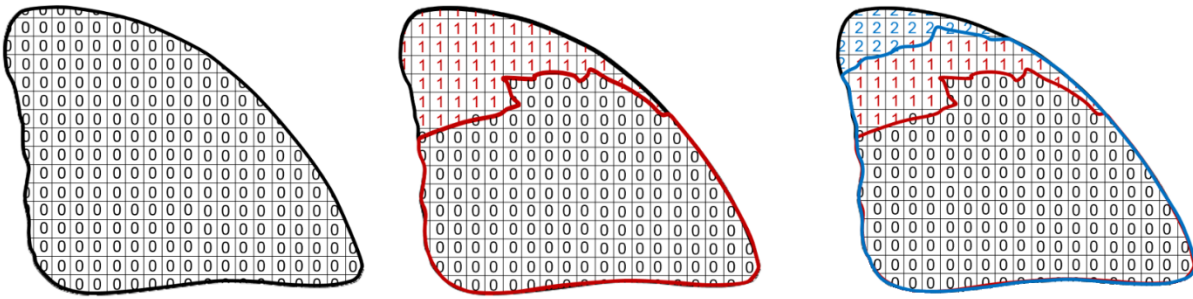


Figure S2. Method used to generate a heat map describing variation in wing damage. Using the mean shape of intact wings as a template (A), we superimposed damaged wings on the intact one by fitting the corresponding undamaged wing outlines (B and C). After each superimposition, missing wing area were counted at the pixel scale. The pixel matrix shown here is at very low resolution for the sake of simplicity. Note that the natural shape variation between individuals (i.e. not due to wing damage) was eliminated so as to match the intact template.

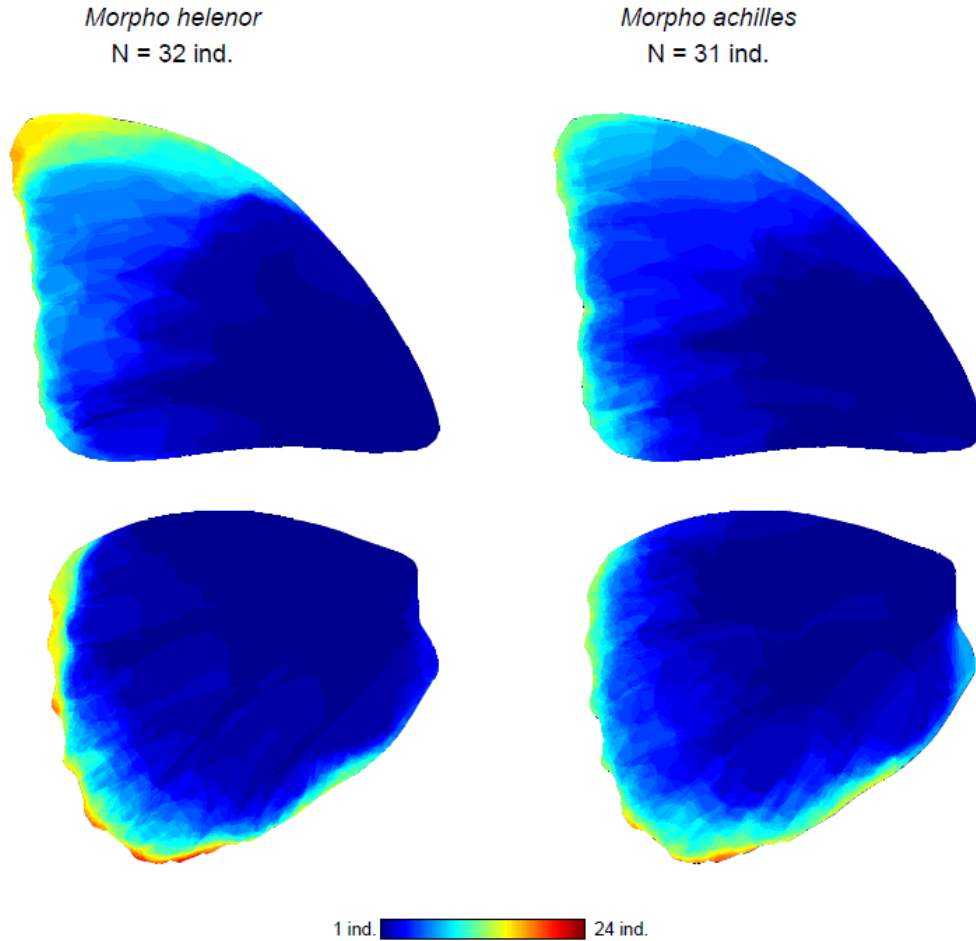


Figure S3. Heat map describing variation in spatial location of wing damage. Left: *Morpho helenor*. Right: *Morpho achilles*. Left and right wings are pooled together for each wing pair. Most frequent damages are in dark red.

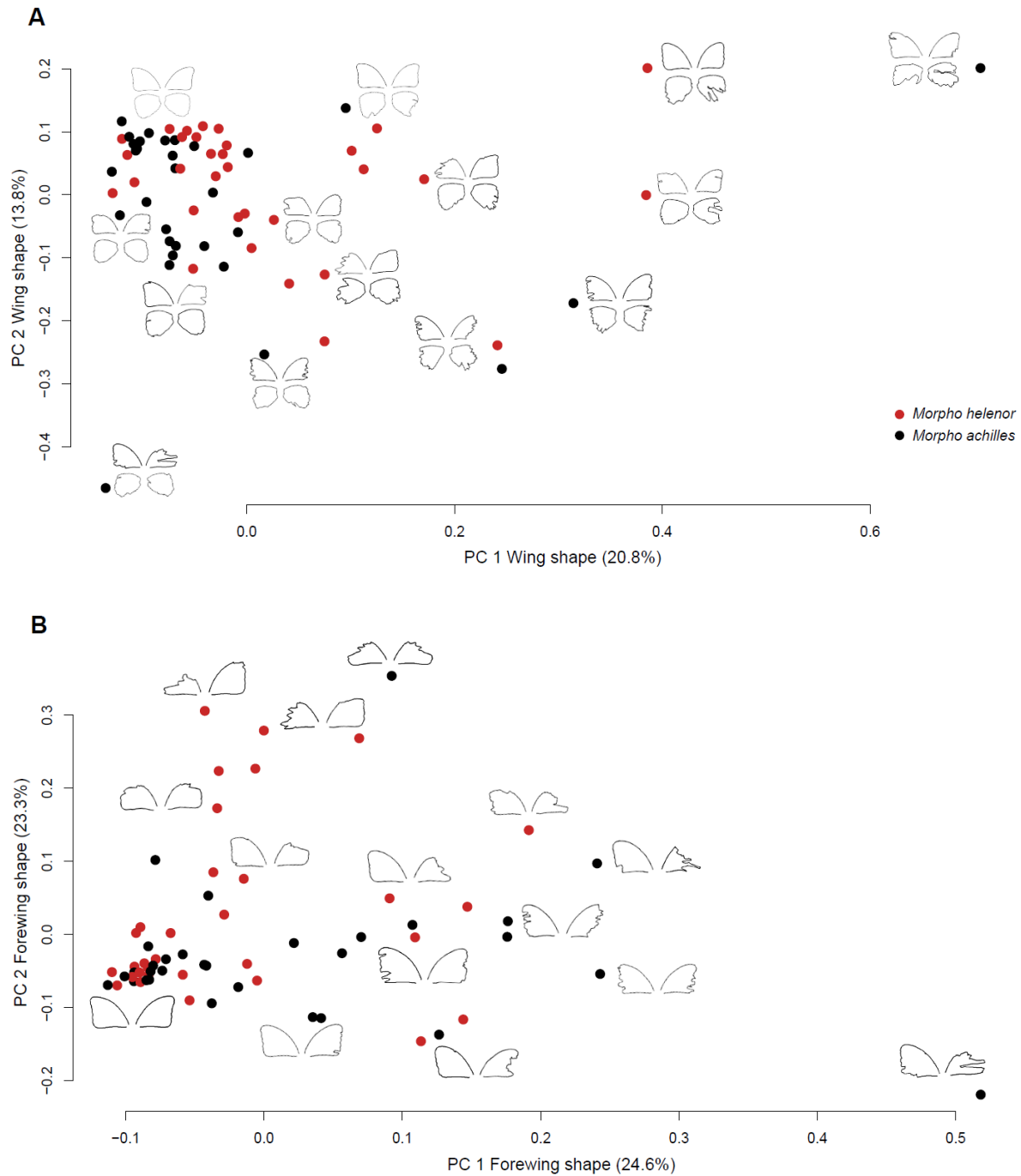


Figure S4. PCA performed on wing outline coordinates. Variation in wing shape among individuals is shown along the two first axes of the PCA. (A) Shape variation when both wing pairs are considered. (B) Shape variation of the forewing pair only is considered. While no clear pattern emerges from the PCA considering both wing pairs, the PCA focusing on forewing shape distinguishes damage occurring mostly on the wing margin along the PC 1 and damage occurring mostly on the upper wing part along PC 2.

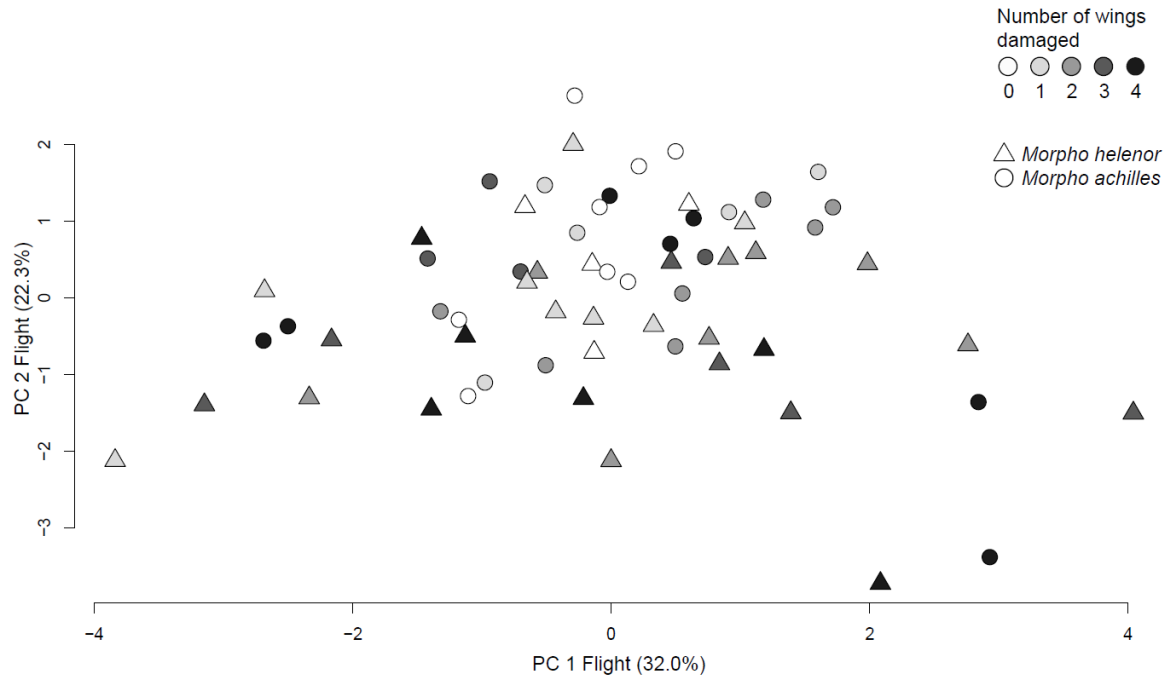


Figure S5. PCA performed on flight parameters. Variation in flight parameters among individuals is shown along the two first axes of the PCA. Triangles and circles represent *Morpho helenor* and *Morpho achilles* respectively. Shades of grey indicate the number of wings damaged at a threshold of >5% of wing area loss. See table S1 for variation in flight parameters along the PCs.

Table S1. Results of Principal Component Analysis on flight parameters.

Axis	1	2	3	4	5	6	7
Percentage of variation explained	32.03	22.26	14.83	11.53	10.02	5.73	3.57
Loadings:							
Wingbeat frequency	0.463	0.372	0.016	0.071	0.368	0.711	0.023
Flight speed	-0.283	0.548	-0.267	0.276	0.426	-0.332	-0.424
Flapping duration	0.555	-0.246	-0.196	-0.168	-0.144	-0.114	-0.729
Flight height	0.336	0.294	0.212	0.669	-0.520	-0.178	0.075
Sinuosity	0.155	-0.328	-0.781	0.363	0.117	-0.020	0.335
Smallest angle	-0.191	0.445	-0.483	-0.343	-0.596	0.246	-0.008
Gliding proportion	-0.473	-0.330	0.035	0.439	-0.152	0.528	-0.413